Metabolic Engineering 12 (2010) 537–551

Contents lists available at ScienceDirect

Metabolic Engineering

journal homepage: www.elsevier.com/locate/ymben

Metabolome, transcriptome and metabolic flux analysis of arabinose fermentation by engineered *Saccharomyces cerevisiae*

H. Wouter Wisselink [a,b], Chiara Cipollina [a,b,1], Bart Oud [a,b], Barbara Crimi [a,b], Joseph J. Heijnen [a,b], Jack T. Pronk [a,b], Antonius J.A. van Maris [a,b,*]

[a] Department of Biotechnology, Delft University of Technology, Julianalaan 67, 2628 BC Delft, The Netherlands
[b] Kluyver Centre for Genomics of Industrial Fermentation, P.O. Box 5057, 2600 GA Delft, The Netherlands

ARTICLE INFO

Article history:
Received 9 April 2010
Received in revised form
16 July 2010
Accepted 26 August 2010
Available online 8 September 2010

Keywords:
Saccharomyces cerevisiae
Evolutionary engineering
Arabinose
Transcriptomics
Metabolomics
Metabolic flux analysis

ABSTRACT

One of the challenges in strain improvement by evolutionary engineering is to subsequently determine the molecular basis of the improved properties that were enriched from the natural genetic variation during the selective conditions. This study focuses on *Saccharomyces cerevisiae* IMS0002 which, after metabolic and evolutionary engineering, ferments the pentose sugar arabinose. Glucose- and arabinose-limited anaerobic chemostat cultures of IMS0002 and its non-evolved ancestor were subjected to transcriptome analysis, intracellular metabolite measurements and metabolic flux analysis. Increased expression of the GAL-regulon and deletion of *GAL2* in IMS0002 confirmed that the galactose transporter is essential for growth on arabinose. Elevated intracellular concentrations of pentose-phosphate-pathway intermediates and upregulation of *TKL2* and *YGR043c* (encoding transketolase and transaldolase isoenzymes) suggested an involvement of these genes in flux-controlling reactions in arabinose fermentation. Indeed, deletion of these genes in IMS0002 caused a 21% reduction of the maximum specific growth rate on arabinose.

1. Introduction

Fermentation of lignocellulosic hydrolysates is a promising strategy for environmentally sustainable and cost-effective production of fuel ethanol from plant biomass (Aristidou and Penttilä, 2000). For economical feasibility at the industrial scale, also smaller carbohydrate fractions of lignocellulosic hydrolysates, such as L-arabinose, need to be converted at high yields and rates together with the most abundant sugars, such as glucose and xylose (Hahn-Hägerdal et al., 2007).

Saccharomyces cerevisiae, currently the organism of choice for fermentative production of ethanol in industry, ferments hexoses at high rates and yields, but wild-type strains cannot grow on the pentose sugars xylose and arabinose. Large efforts have been made to expand its substrate range to include these sugars (Hahn-Hägerdal et al., 2007; Jeffries and Jin, 2004; van Maris et al., 2007). Research initially focused on xylose, the most abundant pentose in plant biomass. By expression of either yeast xylose reductase and xylitol dehydrogenase (XR/XDH) genes or a heterologous xylose isomerase gene, combined with further metabolic and evolutionary engineering approaches, *S. cerevisiae* strains capable of rapidly fermenting xylose have been developed (Jeppsson et al., 2002; Kuyper et al., 2005a; Sedlak and Ho, 2004; Sonderegger and Sauer, 2003). For arabinose fermentation, both bacterial and fungal arabinose utilization pathways have been introduced in *S. cerevisiae* (Becker and Boles, 2003; Bera et al., 2010; Bettiga et al., 2009; Richard et al., 2003; Sedlak and Ho, 2001).

S. cerevisiae IMS0002, the first *S. cerevisiae* strain capable of efficient, fully anaerobic growth and ethanol production on arabinose, was based on expression of the L-arabinose pathway from *Lactobacillus plantarum* in a *S. cerevisiae* strain that had previously been engineered and evolved for xylose fermentation (Kuyper et al., 2005a). In addition to targeted genetic modification, efficient arabinose fermentation required extensive evolutionary engineering in sequential batch cultures grown on L-arabinose (Wisselink et al., 2007).

Evolutionary engineering is a powerful approach for improving industrially relevant properties of microorganisms. However,

Abbreviations: PPP, pentose phosphate pathway; TCA, tricarboxylic acid; G6P, glucose-6-phosphate; F6P, fructose-6-phosphate; T6P, trehalose-6-phosphate; G1P, glucose-1-phosphate; F1, 6BP, fructose-1,6-bisphosphate; PYR, pyruvate; 2, 3PG, 2- and 3-phosphoglycerate; PEP, phosphoenol pyruvate; R5P, ribose-5-phosphate; RBU5P, ribulose-5-phosphate; X5P, xylulose-5-phosphate; S7P, sedoheptulose-7-phosphate; RBU, ribulose; E4P, erythrose-4-phosphate; GAP, glyceraldehyde-3-phosphate; DHAP, dihydroxyacetone phosphate; PYR, pyruvate; FUM, fumarate; SUC, succinate; MAL, malate; OXG, oxoglutarate; CIT, citrate; AcCoA, acetyl-CoA; OAA, oxaloacetate; AcALD, acetaldehyde

* Corresponding author at: Department of Biotechnology, Delft University of Technology, Julianalaan 67, 2628 BC Delft, The Netherlands. Fax: +31 15 278 2355.
E-mail address: A.J.A.vanMaris@TUDelft.NL (A.J. van Maris).
[1] Present address: University of Pittsburgh, Department of Pharmacology and Chemical Biology, 200 Lothrop Street E1314, Pittsburgh, PA 15261, USA.

1096-7176/$ - see front matter © 2010 Elsevier Inc. All rights reserved.
doi:10.1016/j.ymben.2010.08.003

once improved strains have been isolated, identification of the genetic and metabolic changes responsible for the new phenotypes is challenging. In this, chemostat cultures offer clear advantages for comparative analysis of evolved and parental strains because they enable tight control of specific growth rate and other culture parameters. Thus, changes in metabolism or gene expression can be more clearly attributed to the strain background or carbon source (Daran-Lapujade et al., 2009).

Several physiological and molecular studies, using either chemostat or batch cultivation, have been performed on (evolved) xylose-fermenting strains expressing XR and XDH. Many of the observed changes in gene expression were linked to NADPH and NAD^+ metabolism, probably as a consequence of redox constraints imposed upon the engineered cells by the non-matching cofactor preferences of XR and XDH (Jin et al., 2004; Pitkänen et al., 2003, 2005; Sonderegger et al., 2004; Wahlbom et al., 2001, 2003; Zaldivar et al., 2002).

In contrast to XR/XDH-based pathways for xylose fermentation, the bacterial arabinose pathway in *S. cerevisiae* IMS0002 does not impose redox cofactor constraints (Wisselink et al., 2007) and ethanol and carbon dioxide yields are the same for glucose and arabinose. Nevertheless, although major differences between growth on glucose and arabinose can be anticipated in catabolism and in sugar transport, changes in metabolism and gene expression in arabinose-fermenting *S. cerevisiae* strains have not been studied in detail.

The aim of the present study is to identify key genetic changes contributing to efficient arabinose utilization by the evolutionary engineered *S. cerevisiae* strain IMS0002. To this end, strain IMS0002 and its non-evolved ancestor IMS0001 were characterized during anaerobic growth in chemostat cultures, by a combination of transcriptome analysis, extensive intracellular metabolite measurements and metabolic flux analysis. Hypotheses generated by this integrated analysis were tested by deleting involved genes in strain IMS0002.

2. Methods

2.1. Strains and maintenance

S. cerevisiae strains used in this study are listed in Table 1. After addition of 30% (v/v) glycerol, samples from shake-flask cultures were stored in 2 ml aliquots at −80 °C.

2.2. Media and shake-flask cultivation

Cultivation in shake flasks and anaerobic fermenters was performed at 30 °C in synthetic medium (MY), containing 5 g l^{-1} $(NH_4)_2SO_4$, 3 g l^{-1} KH_2PO_4, 0.5 g l^{-1} $MgSO_4 \cdot 7H_2O$, 0.05 ml l^{-1} silicon antifoam and trace elements (Verduyn et al., 1992). For shake flask cultivation, medium pH was adjusted to 6.0 with 2 M KOH prior to sterilization. After heat sterilization (121 °C, 20 min), a filter-sterilized vitamin solution (Verduyn et al., 1992) and sugar(s) were added. Shake-flask cultures were prepared by inoculating 100 ml medium containing the appropriate sugar with a frozen stock culture, and were incubated at 30 °C in an orbital shaker (200 rpm). Solid MY plates containing 20 g l^{-1} glucose (MYG) were prepared by adding 2% agar. Plates were incubated at 30 °C until growth was observed.

2.3. Anaerobic chemostat cultivation

Anaerobic chemostat cultivation was carried out at 30 °C in 2 l fermenters (Applikon, Schiedam, the Netherlands) with a working volume of 1 l. Cultures were performed in MY supplemented with 0.01 g l^{-1} ergosterol and 0.42 g l^{-1} Tween 80 dissolved in ethanol (Andreasen and Stier, 1953, 1954), silicon antifoam, vitamin solution and trace elements (Verduyn et al., 1992), and 20 g l^{-1} glucose (MYG) or arabinose (MYA), and was maintained at pH 5.0 by automatic addition of 2 M KOH. Cultures were stirred at 800 rpm and sparged with 0.5 l min^{-1} nitrogen gas (<10 ppm oxygen). To minimize oxygen diffusion, fermenters were equipped with Norprene tubing (Cole Palmer Instrument Company, Vernon Hills, USA). Absence of oxygen was verified with an oxygen electrode (Applisens, Schiedam, the Netherlands). After inoculation and completion of the batch phase, chemostat cultivation on MYA or MYG was initiated at a dilution rate of 0.03 h^{-1}. The working volume of the culture was kept constant using an effluent pump controlled by an electric level sensor. Chemostats were assumed to be in steady state when, after at least five volume changes, dry weight and specific CO_2 production rate changed by less than 2% over two further volume changes. Samples for microarray, biomass dry weight, extra- and intracellular metabolite analyses were taken between 7 and 9 volume changes after the onset of continuous cultivation.

Table 1
S. cerevisiae strains constructed and used in this study.

Strain	Characteristics	Reference
IMS0001	*MATa ura3-52 HIS3 leu2-3,112 TRP1 MAL2-8c SUC2 loxP-P_{TPI}::(−266, −1)TAL1 gre3::hphMX pUGP$_{TPI}$-TKL1 pUGP$_{TPI}$-RPE1 loxP-P_{TPI}::(−40, −1)RKI1* {pRW231, pRW243} Strain constructed for growth on arabinose,; promoters of *TKL1*, *TAL1*, *RPE1* and *RKI1* replaced by strong *TPI* promoter; transformed with plasmids pRW231 and pRW243, containing *Lactobacillus plantarum AraA*, *AraB* and *AraD*	Wisselink et al. (2007)
IMS0002	As IMS0001; selected for anaerobic growth on L-arabinose	Wisselink et al. (2007)
IMS0012	As IMS0002; *gal2Δ::loxP-KanMX-loxP*	This work
IMS0013	As IMS0002; *ygr043cΔ::loxP-KanMX-loxP*	This work
IMS0014	As IMS0002; *tkl2Δ::loxP-KanMX-loxP*	This work
IMS0019	As IMS0002; *ygr043cΔ::loxP*	This work
IMS0020	As IMS0002; *ygr043cΔ::loxP (1-516)ygr043c::loxP-KanMX-loxP*	This work
IMS0021	As IMS0002; *ygr043cΔ::loxP (1-516)ygr043c::loxP*	This work
IMS0022	As IMS0002; *ygr043cΔ::loxP (1-516)ygr043c::loxP tkl2Δ::loxP-KanMX-loxP*	This work

2.4. Anaerobic sequential batch cultivation

Inocula for anaerobic batch cultures were pregrown at 30 °C in shake flasks containing MYG or MYA. Anaerobic sequential batch cultures of IMS0002 deletion mutants were performed in 1 l of MYA or MYG, using similar fermenter setup and settings as for chemostat cultivation. New cycles of batch cultivation were initiated by manually or computer-controlled replacement of ca. 98% of the culture with fresh medium. In each cycle, maximum specific growth rate was estimated from the CO_2 production profile in the exponential growth phase. To determine the probability (p) that the observed specific growth rates for different IMS0002 deletion mutants were identical, an unpaired Student's T-test was performed, assuming a two-tailed distribution and equal variances. For p-values below a threshold of 0.05, the growth rates were considered significantly different.

2.5. Biomass, carbon dioxide and extracellular metabolite analysis

For biomass dry weight determination culture samples (10.0 ml) were filtered over pre-weighed nitrocellulose filters (pore size 0.45 μm; Gelman laboratory, Ann Arbor, USA). After filtration, the biomass was washed with demineralized water, dried in a microwave oven for 20 min at 360 W and weighed. Duplicate determinations varied by less than 1%.

Exhaust gas from anaerobic fermenters was cooled in a condenser (2 °C) and dried with a Permapure dryer type MD-110-48 P-4 (Permapure, Toms River, USA). Carbon dioxide concentrations were determined with a NGA 2000 analyzer (Rosemount Analytical, Orrville, USA). Exhaust gas flow rates and specific carbon dioxide production rates were determined as described previously (van Urk et al., 1988; Weusthuis et al., 1994).

Glucose, arabinose, acetate, lactate, succinate, glycerol and ethanol were analyzed by HPLC using a Waters Alliance 2690 HPLC (Waters, Milford, USA) supplied with a BioRad HPX 87H column (BioRad, Hercules, USA), a Waters 2410 refractive-index detector and a Waters 2487 UV detector. The column was eluted at 60 °C with 0.5 g l^{-1} sulfuric acid at a flow rate of 0.6 ml min^{-1}.

Carbon recoveries were calculated as carbon in products formed, divided by the amount of sugar carbon consumed, and were based on a biomass carbon content of 48 wt%. To correct for ethanol evaporation in chemostat cultures, the amount of ethanol produced was assumed to equal the measured cumulative production of CO_2 minus the CO_2 production due to biomass synthesis (5.85 mmol CO_2 per gram biomass (Verduyn et al., 1990)) and to acetate formation.

2.6. Metabolic flux distribution

Intracellular metabolic fluxes were calculated through metabolic flux balancing using a compartmented stoichiometric model that was previously developed for describing aerobic growth on glucose (Daran-Lapujade et al., 2004; Lange, 2002) and modified to describe anaerobic growth on glucose and arabinose. Reactions required for production and excretion of organic acids and for transport of oleate and palmitoleate (required for lipid biosynthesis) and the fumarate reductase reaction (TCA reductive branch) were introduced (Daran-Lapujade et al., 2004; Enomoto et al., 2002). Four reactions necessary for arabinose utilization were added to the model: arabinose transport, arabinose isomerase, L-ribulokinase and L-ribulose-5-phosphate-4-epimerase. The assumed macromolecular biomass composition was 45% (w/w) protein, 40.7% (w/w) polysaccharides, 6.3% (w/w) RNA, 0.4% (w/w) DNA, 2.9% (w/w) lipid, 2.5% (w/w) metals, 1.2% (w/w) water, 0.8% (w/w) phosphate and 0.2% (w/w) sulfate (Lange, 2002; Nissen et al., 1997). Measured protein contents of IMS0001 and IMS0002 strains agreed with the assumed value (data not shown). The complete set of reactions and metabolites used in the model is reported in Table S1.

Dedicated software (SPAD it, Nijmegen, The Netherlands) was used for metabolic flux balancing, the theory and practice of which have been thoroughly described elsewhere (Nissen et al., 1997; Vallino and Stephanopoulos, 1990; van Gulik and Heijnen, 1995) and will not be repeated here. For each growth condition, specific rates of growth, substrate consumption and carbon-dioxide, glycerol, acetate, pyruvate, lactate and succinate production were measured. For the conversion of fluxes into mmoles per Cmole of biomass, a biomass C-molar weight of 25.87 g mol^{-1} was used (Lange, 2002; Nissen et al., 1997). The number of measured rates was sufficient to result in an over-determined system, thus enabling data reconciliation. In all cases the degree of redundancy equaled 2.

2.7. Intracellular metabolites

Sampling and sample preparation for analysis of intracellular metabolite concentrations was carried out as previously described (Mashego et al., 2004). In total 1 ml of broth was rapidly quenched in 5 ml of −40 °C 60% (vol/vol) aqueous methanol. After centrifugation (2000*g*, −20 °C, 5 min), the pellet was resuspended in 5 ml of −40 °C 60% (vol/vol) aqueous methanol and centrifuged again. Intracellular metabolites were extracted from the pellet with boiling 75% (vol/vol) aqueous ethanol. The ethanol extracts were evaporated to dryness, resuspended in 0.5 ml de-ionized water and centrifuged (13,000*g*, 4 °C, 5 min). Supernatants were stored at −80 °C until further analysis.

Concentrations of G6P, F6P, T6P, G1P, F1,6BP, PYR, 2,3PG, PEP and the TCA cycle intermediates FUM, SUC, MAL, OXG and CIT in the cell extracts were analyzed by liquid chromatography-electrospray ionization-tandem mass spectrometry (LC-ESI-MS/MS) according to Van Dam et al. (2002). 2PG and 3PG could not be resolved with this procedure, so their sum was determined. Metabolite quantification was performed by the Isotope Dilution Method (IDMS) (Wu et al., 2005). Intracellular concentrations of the PPP intermediates R5P, RBU5P, X5P, S7P, E4P, and RBU, GAP and DHAP were determined with a recently described GC-IDMS method (Cipollina et al., 2009). Chemicals were purchased from Sigma-Aldrich, Pierce and Glycoteam. L-Ribulose was kindly provided by Prof. Wim Soetaert, Department of Biochemical and Microbial Technology, Ghent University, Belgium. Intracellular concentrations of adenine nucleotides (AMP, ADP and ATP) were quantified by LC-ESI-MS/MS (Seifar et al., 2009). Cellular energy charge was calculated from the adenine nucleotide concentrations according to

$$\frac{[ATP]+\frac{1}{2}[ADP]}{[ATP]+[ADP]+[AMP]} \quad (1)$$

Concentrations of free amino acids in cell extracts were determined using a Trace GC Ultra coupled to a Trace DSQ Mass Spectrometer (Finnigan, MA, USA). Solid phase extraction of the amino acids was carried out using the EZ:faast kit (Phenomenex, Torrance, CA, USA) (Nasution et al., 2008).

2.8. Microarray processing and analysis

Sampling from chemostat cultures and total RNA extraction was performed as previously described (Piper et al., 2002). Probe preparation and hybridization to Affymetrix Genechip YG-S98 microarrays were performed according to Affymetrix instructions, with the following modifications: double-stranded cDNA synthesis was carried out using 15 μg of total RNA and the components of the One Cycle cDNA Synthesis Kit (Affymetrix). The double-stranded cDNA was purified (Genechip Sample Cleanup Module, Qiagen) before *in vitro* transcription and labeling (GeneChip IVT Labeling Kit, Affymetrix). Finally, labeled cRNA was purified (GeneChip Sample Cleanup Module) prior to fragmentation and hybridization of 15 μg of biotinylated cRNA. The quality of total RNA, cDNA, cRNA and fragmented cRNA was monitored using the Agilent Bioanalyser 2100 (Agilent Technologies). Acquisition and quantification of array images and data filtering were performed using Affymetrix GeneChip® Operating Software (GCOS) version 1.2. Prior to comparison, all arrays were globally scaled to a target value of 150, using the average signal from all gene features, with GCOS (version 1.2). From 9335 transcript features on the YG-S98 arrays, a filter was applied to extract 6383 yeast ORFs (Boer et al., 2003). To eliminate insignificant variations, genes with expression values below 12 were set to 12. Genes whose maximum expression was 12 over the 9 arrays, and genes whose average

expression levels was less than 20 over the 9 arrays were discarded. To indicate the variation in triplicate measurements, the coefficient of variation (CV, standard deviation divided by the mean) was calculated for each probe set, after which the average CV was determined for each condition.

For statistical pair-wise comparisons of the two strains and growth conditions, Microsoft Excel running the Significance Analysis of Microarrays (SAM, version 2.21) add-in was used. Applying an expected false discovery rate (FDR) of at most 1% and a fold change (FC) of 2, genes with significantly changed expression levels were identified. Clusters of up- or down regulated genes were analyzed for enrichment in functional annotation and significant transcription factor binding (Harbison et al., 2004) as described before (Knijnenburg et al., 2007). Functional annotations were derived from the MIPS Functional Catalogue Database (FunCatDB, www.helmholtz-muenchen.de).

2.9. Gene deletion in the IMS0002 background

Gene deletion in IMS0002 was achieved by integration of a G418 resistance cassette replacing the target gene. For the deletion of *GAL2*, *TKL2* and *YGR043C*, the *KanMX* cassette from pUG6 was amplified by PCR (Güldener et al., 1996), using oligonucleotides indicated in Table 2. For the deletion of *TKL2* in the Δ/Δ*ygr043c* strain IMS0020, a *KanMX TKL2* disruption cassette of approximately 2500 bp was amplified using IMS0014 (Δ*tkl2*) genomic DNA as a template. After purification of the PCR products (GenElute PCR Clean-up Kit, Sigma, Steinheim, Germany), overnight cultures of strain IMS0002 were transformed (Gietz and Woods, 2002) with the gene disruption cassette. Transformed cells were selected on MYG-agar containing 200 μg ml^{-1} G418 (InvivoGen, San Diego, USA). Correct integration of the *KanMX* cassette was verified by PCR on single colonies using diagnostic oligonucleotides that bind to the *KanMX* cassette and regions up- and downstream of the target gene (Table 2).

For multiple gene deletions, the *KanMX* marker was rescued before deleting the next target gene. To this end, cells were transformed with pSH65, expressing the inducible Cre-recombinase and carrying the phleomycin resistance gene *ble*^{r} (Güldener et al., 2002). Transformed cells were spread on MYG plates containing phleomycin and incubated at 30 °C until colonies appeared. Liquid MYG containing 7.5 μg/ml phleomycin (InvivoGen, San Diego, USA) was inoculated with several phleomycin resistant colonies, incubated overnight at 30 °C for induction of the-Cre recombinase, and transferred to solid MYG with phleomycin. Removal of the *KanMX* cassette by the Cre-recombinase was confirmed by replica plating of phleomycin-resistant yeast colonies on MYG and MYG-G418 and by diagnostic PCR on single colonies that had lost G418 resistance. Subsequently, loss of pSH65 was achieved by growing cells non-selectively for 5–10 generations in MYG without phleomycin, after which loss of phleomycin resistance was confirmed by replica plating of single colonies on solid MYG with and without phleomycin.

3. Results

3.1. Physiology of *S. cerevisiae* IMS0001 and IMS0002 in anaerobic glucose- or arabinose-limited chemostat cultures

S. cerevisiae IMS0001, which expresses the arabinose pathway from *L. plantarum*, is unable to grow on arabinose. Extensive evolutionary engineering resulted in strain IMS0002, which can grow anaerobically on arabinose and efficiently ferment it to ethanol (Wisselink et al., 2007). Both strains were grown in anaerobic chemostats, in which growth was limited by either glucose (both strains) or arabinose (only strain IMS0002). The dilution rate was 0.03 h^{-1} for these three situations, taking into account the μ_{max} of strain IMS0002 for anaerobic growth on arabinose of approximately 0.05 h^{-1} (Wisselink et al., 2007).

Table 2
Oligonucleotides used in this study for the construction of gene deletions. A KanMX gene deletion cassette was obtained by PCR by using combinations of the DisA and DisB oligonucleotides. Genes were disrupted by homologous recombination between the target gene and the KanMX gene deletion cassette. Recombination sites are indicated by the underlined regions in the oligonucleotides. Deletion or disruption was confirmed by PCR using diagnostic primers KanA and KanB combined with, depending on the orientation of the KanMX cassette in the target locus, either the FW or the RV primer corresponding with the target gene (e.g. KanA combined with Tkl2-FW and KanB combined with Tkl2-RV).

Name	5′–3′ DNA sequence
Oligos used for construction of gene disruption cassettes	
Gal2-disA	TAAGTAAACACAAGATTAACATAATAAAAAAAATAATTCTTTCATAGCATAGGCCACTAGTGGATCTG
Gal2-disB	TAAGAGAGATGATGGAGCGTCTCACTTCAAACGCATTATTCCAGCTGAAGCTTCGTACGC
Tkl2-disA	TCTACGTAGACGATTATACCTTACTAATCAAAAAAAGAACACAGCTGAAGCTTCGTACGC
Tkl2-disB	GTGACCATCAACCAGGAAGTGTGAAATAGCAAAGAACTGTGCATAGGCCACTAGTGGATCTG
Ygr043c-disA	AGCGTAAGTCATAAAAAATAGGAAATAATCACATATATACAAGCAGCTGAAGCTTCGTACGC
Ygr043c-disB	ATATATTTATATATATAAGTAGGTACCTCTACTCTTAATGGCATAGGCCACTAGTGGATCTG
Ygr043c-disC[a]	AAACAGTAATGTCATATTACAATGAATACCATGCTTTACTTGCATAGGCCACTAGTGGATCTG
TKL2dis500FW[b]	TCTTAATGGTGGCTCGCTGTC
TKL2dis500RV[b]	TCAATGCAGCCCATACACTC
Oligos used for diagnostic purposes	
KanA	CGCACGTCAAGACTGTCAAG
KanB	TCGTATGTGAATGCTGGTCG
Gal2-FW	ATGGCATTATACTCCTGCTAGAAAG
Gal2-RV	AAAGGATGGCAGAGCATGTTATCG
Tkl2-FW	TAATGGTGGCTCGCTGTCTC
Tkl2-RV	CCCAGCGGGTCTTCAAATAC
Ygr043c-FW	ACAGTCGGTCTGGGTTGAAG
Ygr043c-RV	GCCTTTCAAGAAGCCCAAGAG
TKL2dis700FW[b]	CGCCTACGCTTGACATCTAC
TKL2dis700RV[b]	GGCCAAACGGAACAACTGAG

[a] Ygr043c-disC was used in combination with Ygr043c-disA to make the second *YGR043C* deletion in IMS0019, resulting in strain IMS0020.
[b] These primers were used for the construction and confirmation of the *TKL2* deletion in strain IMS0021, resulting in strain IMS0022.

In the anaerobic glucose- and arabinose-limited chemostat cultures, alcoholic fermentation provided the free energy required for biosynthesis and maintenance (Table 3). Due to reoxidation of excess NADH from biosynthesis (van Dijken and Scheffers, 1986), similar amounts of glycerol were formed under all three conditions tested. With the exception of a lower acetate production rate in strain IMS0001, specific rates of (by)product formation were very similar in all three situations (Table 3). Due to the impact of cellular maintenance at low specific growth rate, the biomass yield on substrate (Y_{sx}) of the cultures was only 0.066 ± 0.001 g g^{-1} for IMS0001, and a slightly higher yield of 0.072 ± 0.003 and 0.075 ± 0.001 g g^{-1} for glucose- and arabinose-limited growth of IMS0002, respectively (Table 3). The differences in biomass yield might be explained by small differences in biomass composition and storage carbohydrates. Furthermore, the residual concentration of arabinose (23.4 ± 1.2 mmol l^{-1}) was much higher than that of glucose (< 0.5 mmol l^{-1}), indicating a low affinity for arabinose, as previously observed in batch cultivations on arabinose of strain IMS0002 (Wisselink et al., 2007).

Based on the measured external consumption and production rates (Table 3) the distribution of intracellular fluxes was calculated with a stoichiometric model (Fig. 1 and Supplementary Table S1). In glucose-limited cultures, overall flux distribution was highly similar for the two strains. Glycolysis was the main catabolic route and only a small fraction of the carbon flux, dictated by biosynthetic requirements, was directed to the pentose phosphate pathway (PPP; Fig. 1). Comparison of flux distribution in glucose- and arabinose-limited cultures revealed major differences, especially in upper glycolysis and in the PPP (Fig. 1). During growth on arabinose, the non-oxidative part of the PPP functions as major catabolic pathway by converting X5P into the glycolytic intermediates F6P and GAP. Consequently, the flux through the non-oxidative PPP was about 30-fold higher than during glucose-limited growth. In arabinose-grown cultures, some F6P was converted into G6P and channeled into the oxidative PPP for NADPH generation (Fig. 1). Accordingly, the calculated flux through glucose-6-phosphate isomerase during growth on arabinose proceeded in the reverse direction and at a 15-fold lower rate than during growth on glucose. The D-ribulose-5-phosphate epimerase reaction also proceeded in opposite directions during growth on arabinose compared to glucose. Consistent with the measured external rates, fluxes through the lower part of glycolysis, tricarboxylic acid (TCA) cycle and biosynthetic pathways were highly similar in all three situations (Fig. 1).

3.2. Transcriptome analysis: data quality and global responses

Transcriptome analysis was performed with oligonucleotide arrays, yielding average coefficients of variation ranging from 10% to 14% for data from independent triplicate cultures for each of the three situations tested. Pairwise comparison between the three situations yielded 575 genes in total, divided over 6 clusters, which showed a minimum two-fold statistically significant difference in one of the three situations compared to the others (Fig. 2).

Among the total of 298 genes that showed a higher transcript level in the evolved strain IMS0002 than in the parental strain IMS0001 (clusters I, II, III, IV and VI), 24% represent genes on chromosome VII. Virtually all of these are located on a 250 kb region of chromosome VII (Fig. 3), which is a strong indication for duplication of this region during selection for improved arabinose fermentation. Strong support for this was found during construction of a Δ*ygr043c* IMS0002 strain. The presence of two copies of *YGR043c* in IMS0002, a gene that is located in the 250 kb region (Fig. 3), was confirmed by diagnostic PCR.

Overrepresentation of functional categories and transcription-factor binding sites among the six gene clusters was studied by hypergeometric distribution analysis (Fig. 2). Amongst genes that showed an increased transcript levels for the three comparisons, three unique transcription-factor binding sites were overrepresented. In addition to this, 9 MIPS categories were overrepresented, comprising genes encoding enzymes involved in the TCA cycle, electron transport and membrane-associated energy conservation, respiration (MIPS categories 02.10, 02.11 and 02.13) and transport (MIPS category 20). Among the genes whose transcript level was lower in strain IMS0002, 13 unique transcription factor binding sites were overrepresented, along with 2 MIPS categories. It seems unlikely that all genes on the putatively duplicated region from chromosome VII are linked to the phenotype of IMS0002. When this group of genes was omitted from the analysis, four additional MIPS categories were identified in clusters I and IV (Fig. 2, Supplementary Table S2), indicating that the duplicated genes affected the hypergeometric distribution.

Genes whose expression was different in comparisons between the two strains, irrespective of the sugar on which strain IMS0002 was grown, made up the largest cluster (cluster I, Fig. 2). In this cluster, no overrepresented functional categories or transcription-factor binding sites were identified among the 131 genes whose transcript levels were higher in the evolved strain. However, when the analysis was repeated without the genes of the duplicated region on chromosome VII the MIPS categories (carbon) metabolism and co-factor binding were shown to be overrepresented (Fig. 2). Among the 117 genes that showed a reduced transcript level in strain IMS0002 (cluster I), binding sites for the Cin5p, Yap6p and Sok2p transcription factors were overrepresented (Supplementary Table S2). Cin5p (Yap4p) and Yap6p are (putative) basic leucine zipper (bZIP) transcription factors of the yAP-1 family that are involved in various biological functions (Fernandes et al., 1997). Sok2p is a nuclear protein that plays a regulatory role in the cyclic AMP (cAMP)-dependent protein kinase (PKA) signal transduction pathway (Ward et al., 1995).

A small number of genes were differentially expressed in arabinose-limited chemostat cultures of IMS0002 compared to the

Table 3
Specific consumption and production rates and other physiological parameters of *S. cerevisiae* strains IMS0001 and IMS0002 during anaerobic glucose- or arabinose-limited chemostat cultures at a dilution rate of 0.03 h^{-1}. The values represent average specific rates of at least triplicate chemostat cultivations ± the standard deviation.

Strain	Carbon limitation	Residual glucose or arabinose (mmol l^{-1})	Specific consumption or production rate (mmoles [Cmole DW]$^{-1}$ h^{-1})								Biomass yield (g g^{-1})[a]	Carbon recovery (%)
			Glucose or arabinose	Ethanol	CO_2	Succinate	Lactate	Glycerol	Acetate	Pyruvate		
IMS0001	Glucose	< 0.5	68.4 ± 0.1	110.6 ± 1.5	115.5 ± 1.5	0.25 ± 0.22	0.22 ± 0.39	7.8 ± 0.3	0.12 ± 0.10	0.03 ± 0.05	0.066 ± 0.001	95.9 ± 1.0
IMS0002	Glucose	< 0.5	61.0 ± 1.9	102.2 ± 5.8	107.2 ± 5.6	0.34 ± 0.02	0.48 ± 0.03	7.4 ± 0.5	0.38 ± 0.04	0.07 ± 0.004	0.072 ± 0.003	100.9 ± 1.8
IMS0002	Arabinose	23.4 ± 1.2	71.6 ± 3.4	97.8 ± 6.7	103.2 ± 6.9	0.33 ± 0.04	0.51 ± 0.03	7.0 ± 0.15	0.63 ± 0.18	0.05 ± 0.04	0.075 ± 0.001	99.3 ± 4.0

[a] Biomass yield is defined as grams of biomass produced per gram of consumed sugar.

glucose-limited cultures of both strains (cluster II, Fig. 2). Of 19 genes whose transcript levels were higher in the arabinose-grown cultures, 12 shared a Gal4p transcription-factor binding site (*GAL1, GAL2, GAL3, GAL7, GAL10, GAL80, GCY1, MLF3, MSK1, PCL10, RIO1* and *YEL057C*). Transcript levels of these genes, of which some are involved in galactose metabolism and are known to be induced by galactose, were 2- to 488-fold higher in arabinose-limited cultures of strain IMS0002 than in glucose-limited cultures. The down-regulated genes in cluster II were enriched for Dig1p, Tec1p, Ste12p and Mcm1p transcription-factor (pair) binding sites and functional categories that

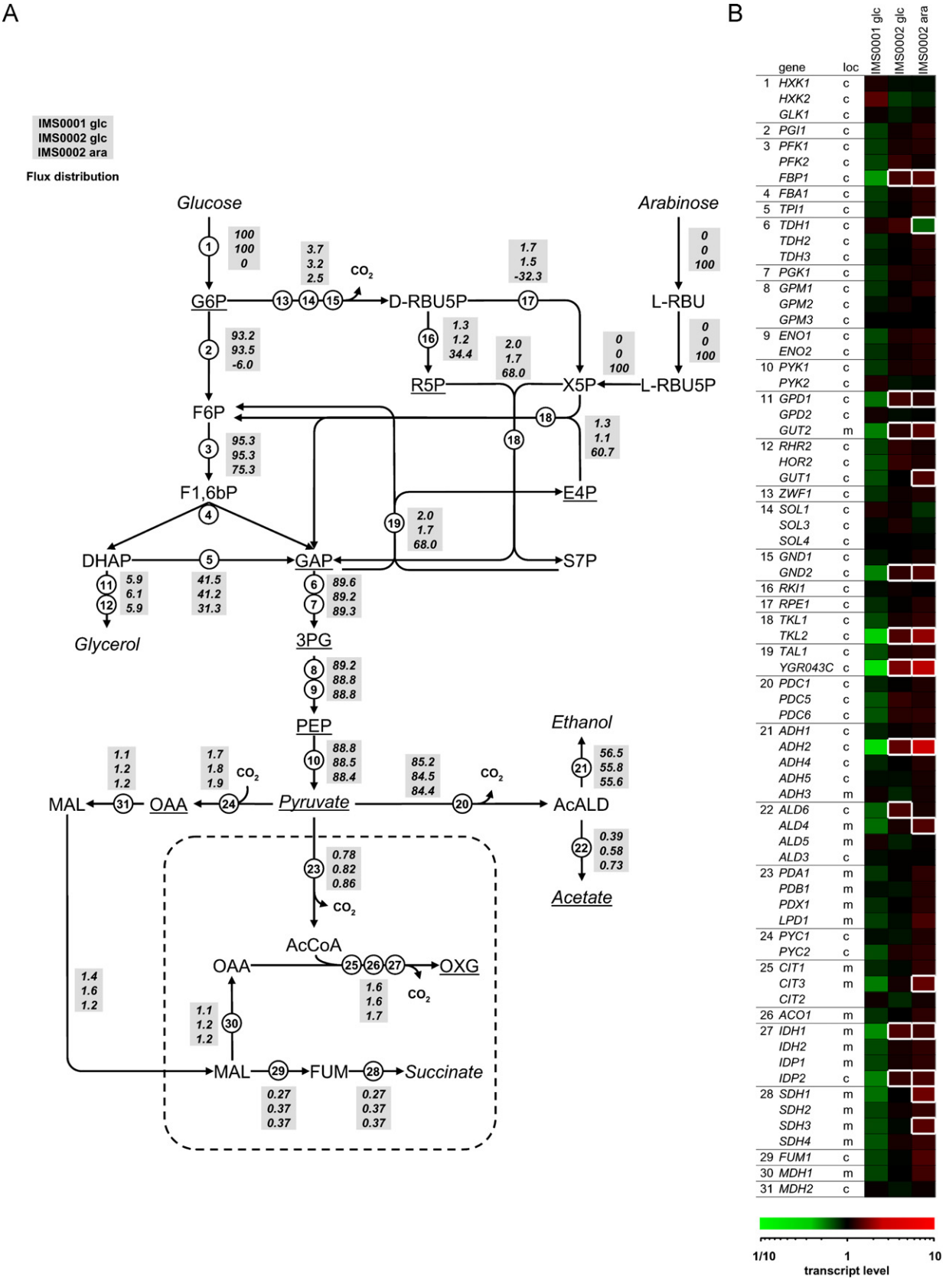

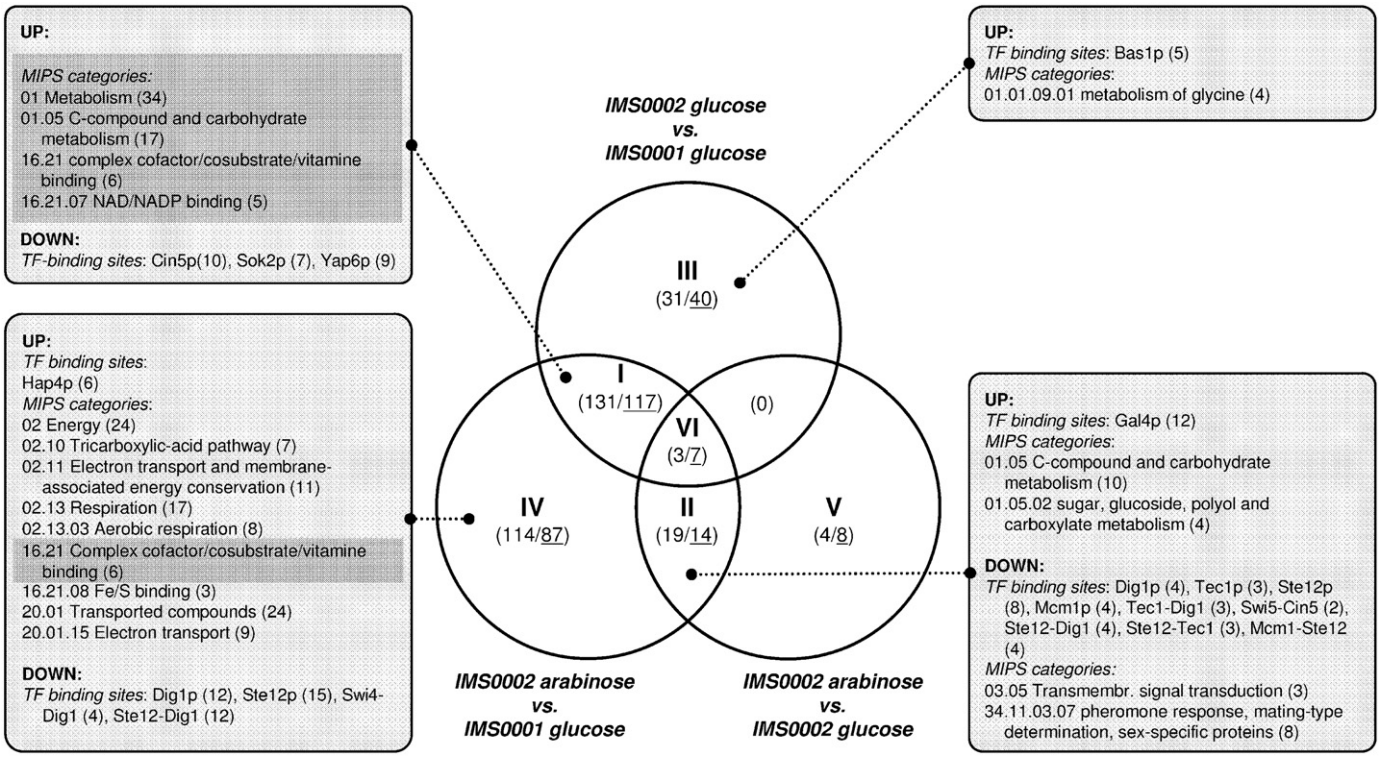

Fig. 2. Venn diagram representing (overlapping) clusters of differentially expressed genes for the comparisons: IMS0002, glucose-limited vs. IMS0001, glucose-limited; IMS0002, arabinose-limited vs. IMS0001, glucose-limited; IMS0002, arabinose-limited vs. IMS0002, glucose-limited. For each cluster the number of up- and down-regulated genes is indicated (regular and underlined numbers in parentheses, respectively). For each cluster hypergeometric distribution analysis was performed to identify overrepresented functional categories of genes and transcription factor (TF) binding sites (light gray boxes). The gray shaded categories were identified when a group of putatively duplicated genes on chromosome VII were omitted from the analysis.

related to pheromone response and sexual reproduction (*AGA1, AGA2, BAR1, FUS1, FUS3, MFA1, MFA2, STE6*). In addition to target genes of Tec1p, the expression level of *TEC1* itself was down-regulated in strain IMS0002 (Table 4). Genes with an overrepresentation of Dig1p and Ste12p binding sites were also observed in cluster IV, which compares arabinose-limited cultures of strain IMS0002 with glucose-limited cultures of strain IMS0001. The enriched functional categories with increased transcript levels in cluster IV (TCA cycle, electron transport and respiration) suggests that a release of catabolite repression may have been responsible for increased transcript levels during growth on arabinose. However, since these genes were not found in a comparison of glucose- and arabinose-limited cultures of strain IMS0002, this response is also affected by the evolutionary engineering of strain IMS0002.

3.3. Differential expression of central carbon metabolism genes

To determine if the observed differences in flux distribution between arabinose- and glucose-limited cultures were reflected in gene expression, transcript levels of genes involved in central carbon metabolism were compared for the three analyzed situations (Fig. 1, Table 4). Transcript levels of nine of these genes were at least two-fold higher in both glucose- and arabinose-limited cultures of IMS0002 than in glucose-limited cultures of its parental strain IMS0001 (Fig. 2, cluster I). Of these nine genes, *TKL2* and *YGR043C* encode isoenzymes of transketolase and transaldolase, respectively (Huang et al., 2008; Schaaff-Gerstenschläger et al., 1993) and are thus related to the non-oxidative PPP. Transcript levels of *TKL2* in glucose- and

Fig. 1. (A) Flux distribution in the central carbon metabolism during anaerobic glucose- or arabinose-limited chemostat cultures of *S. cerevisiae* strains IMS0002 and IMS0001 at a dilution rate of 0.03 h^{-1}. The fluxes were calculated by using a stoichiometric model as described in the methods section. The complete set of reactions in the stoichiometric model is listed in Supplementary Table S1. Fluxes are normalized to a total specific sugar consumption of 100 Cmmoles (Cmoles biomass)$^{-1}$ h^{-1}. Compounds in italics are the ones exchanged with the extra-cellular space, compounds underlined are those used for biomass synthesis. The fluxes in the gray boxes refer to (from top to bottom): IMS0001, glucose-limited; IMS0002, glucose-limited; IMS0002, arabinose-limited. The circled numbers represent the enzymatic reactions implemented in the model and their corresponding genes (B) hexokinase (1), glucose-6-phosphate isomerase (2), phosphofructokinase/fructose-1,6-bisphosphatase (3), fructosebisphosphate aldolase (4), triosephosphate isomerase (5), glyceraldehyde-3-phosphate dehydrogenase (6), phosphoglycerate kinase (7), phosphoglycerate mutase (8), enolase (9), pyruvate kinase (10), glycerol-3-phosphate dehydrogenase (11), glycerol-3-phosphatase/glycerol kinase (12), glucose-6-phosphate dehydrogenase (13), lactonase (14), 6-phosphogluconate dehydrogenase (15), ribose-5-phosphate isomerase (16), ribulose-5-phosphate 3-epimerase (17), transketolase (18), transaldolase (19), pyruvate decarboxylase (20), alcohol dehydrogenase (21), acetaldehyde dehydrogenase (22), pyruvate dehydrogenase (23), pyruvate carboxylase (24), citrate synthase (25), aconitase (26), isocitrate dehydrogenase (27), succinate dehydrogenase (28), fumarase (29), mitochondrial malate dehydrogenase (30), cytosolic malate dehydrogenase (31). (B) Tile visualization of half-Z item-wise normalized transcript levels (Genedata Analyst, Genedata AG, Germany) of genes encoding enzymes involved in the (anaerobic) central carbon metabolism during anaerobic chemostat cultivation of: IMS0001, glucose-limited (IMS0001 glc); IMS0002, glucose-limited (IMS0002 glc); and IMS0002, arabinose-limited (IMS0002 ara). The numbers in the first column correspond to the circled numbers in (A). In the second and the third column the gene(s) encoding the enzymes and their cellular location are indicated (c, cytosol; m, mitochondria). High and low transcript levels are represented by different shades of red and green respectively. Significant changes in transcript level of at least two-fold, compared to the reference condition IMS0001 glc, are indicated by tiles bordered by white lines. (For interpretation of the references to color in this figure legend, the reader is referred to the web version of this article.)

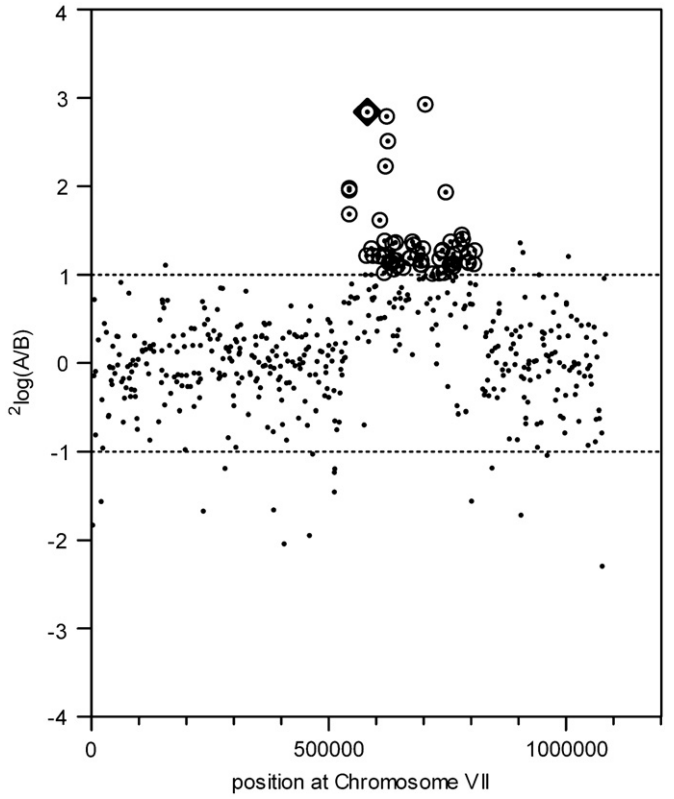

Fig. 3. Comparison between transcript levels of strain IMS0002 and IMS0001, both cultivated anaerobically under glucose-limited conditions, ranked on the start positions of the corresponding genes on chromosome VII. The ^{2}log(*A*/*B*) values represent the ^{2}log of the ratio between the expression levels of IMS0002 (A) and IMS0001 (B). The dotted lines indicate a 2-fold change cut-off for the expression levels. The circled dots represent genes located between positions 543555 and 807659 with a significant up-regulation in expression level of at least 2 fold, The diamond represents the fold-change expression level of *YGR043C*, encoding a transaldolase.

arabinose-limited cultures of strain IMS0002 were 3.9 and 5.5-fold higher, respectively, than in glucose-limited cultures of strain IMS0001 (Table 4). Similarly, the transaldolase-encoding gene *YGR043C*, which is located on the putative duplicated 250 kb region of chromosome VII (Fig. 3), showed 7.2- and 9.7-fold higher transcript levels in the evolved strain (Table 4). *GND2,* which encodes a 6-phosphogluconate dehydrogenase involved in the oxidative part of the PPP, showed significantly higher transcript levels in strain IMS0002.

In line with the modest flux differences in glycolysis, no drastically different transcript levels were observed for genes involved in the upper part of glycolysis (Table 4). Expression levels of the gluconeogenetic gene *FBP1*, encoding fructose-1,6-bisphosphatase, were increased 3-fold. In the lower half of glycolysis, only expression of *TDH1*, which encodes one of three isoenzymes of glyceraldehyde-3-phophate dehydrognease, was significantly reduced under arabinose-limited conditions. In addition, transcript levels of *GPD1* and *GUT2*, which encode cytosolic and mitochondrial glycerol-3-phosphate dehydrogenases, respectively, were increased in strain IMS0002 under both cultivation conditions. *GUT1* (mitochondrial glycerol kinase) and *DAK2* (dihydroxyacetone kinase), both encoding enzymes involved in glycerol metabolism, were also upregulated (Table 4). The up-regulation of *GPD1* and *DAK2,* in addition to the aldo-keto reductases *GCY1* and *YPR1* (Table 4), might indicate adaptation of strain IMS0002 to (osmotic) stress by glycerol dissimilation via the dihydroxyacetone pathway (Norbeck and Blomberg, 1997).

At the pyruvate branch point, a 6- and 10-fold increase of *ADH2* (alcohol dehydrogenase) was observed for strain IMS0002 under glucose- and arabinose-limited conditions, respectively. The expression of two genes encoding acetaldehyde dehydrogenases (*ALD6* and *ALD4*) was significantly increased in only one condition. Hypergeometric distribution analysis showed that genes encoding enzymes of the tricarboxylic acid cycle were overrepresented among the up-regulated genes in cluster IV (Fig. 2). Particularly, *CIT3*, *IDH1*, *IDP2*, *SDH1*, *SDH3*, *LSC2*, *KGD1* and *KGD2* were upregulated under at least one condition (Table 4). In addition, two representatives of the glyoxylate cycle, *ICL1* and *MLS1*, were upregulated at least two-fold for strain IMS0002 grown at both glucose- and arabinose-limited conditions. Both the up-regulation of TCA and glyoxylate cycle genes (Jin et al., 2004) and the acetaldehyde dehydrogenases encoding genes *ALD4* and *ALD6* (Runquist et al., 2009; Salusjärvi et al., 2006), have previously been observed for some xylose consuming strains.

3.4. Increased concentrations of non-oxidative pentose phosphate pathway intermediates during arabinose-limited growth

The fluxes through the non-oxidative PPP were more than 30-fold higher during anaerobic arabinose-limited growth than during glucose-limited growth. To further investigate these different flux distributions and to identify possible rate-controlling reactions in central carbon metabolism during growth of the evolved strain IMS0002 on arabinose, intracellular concentrations of key metabolites from glycolysis, TCA cycle, and PPP were determined. To gage the biosynthetic and energetic status of the cultures, intracellular concentrations of free amino acids and adenine nucleotides were also determined.

In carbon-limited chemostat cultures grown at the same specific growth rate on different substrates that in theory result in the same biomass composition, biosynthetic rates from common precursor metabolites are identical. Although small differences were observed in the biomass yields, the intracellular concentrations of free amino acids, which are key precursors for biosynthesis, did not differ in the three situations tested (data not shown). Adenine nucleotide concentrations (AMP, ADP and ATP) were also similar in all cultures. The adenine nucleotide energy charge, which reflects the overall cellular energy status (Atkinson, 1968), was similar for all three situations (0.81 for glucose-limited cultivation of IMS0001, 0.87 for glucose-limited cultivation of IMS0002 and 0.83 for arabinose-limited cultivation of IMS0002).

As described above, calculated intracellular flux distributions differed strongly for growth on glucose and arabinose. With the exception of 6PG and E4P, intracellular concentrations of PPP intermediates differed considerably for the three analyzed situations. During arabinose-limited growth, concentrations of R5P, X5P, RBU5P and S7P were 2.6-, 6.1-, 6.1- and 16-fold higher, respectively, than during glucose-limited growth (Fig. 4). Although less pronounced, similar differences were observed in a comparison of the two strains grown in glucose-limited cultures, with slightly higher concentration of PPP metabolites in the evolved strain IMS0002. Ribulose was found at a relatively high concentration of 1.4 μmol $(g\,DW)^{-1}$ in arabinose-limited cultures. Unexpectedly, low intracellular concentrations of ribulose were also found in glucose-limited cultures of strain IMS0002. Unfortunately, the recently developed GC–MS method (Cipollina et al., 2009), which enables quantification of the PPP intermediates and ribulose, did not allow us to distinguish between D- and L-enantiomers of RBU5P, metabolites that are both expected to be detected in IMS0002 during arabinose-limited growth (Fig. 1).

Table 4
Transcript levels during anaerobic glucose- and arabinose-limited chemostat cultures of strains IMS0001 and IMS0002 at a dilution rate of 0.03 h^{-1}, for genes encoding hexose transporters, enzymes involved in glycolysis, glycerol metabolism, pentose phosphate pathway, pyruvate branchpoint, TCA cycle, glyoxylate cycle, galactose metabolism, aldo-keto reductases and regulatory proteins. Only the genes that showed at least a significant 2-fold change for at least one condition are shown.

Enzyme/protein	Nr.[a]	Gene	Transcript levels (arbitrary units) ± SD[b]		
			IMS0001 glc	IMS0002 glc	IMS0002 ara
Hexose transporters					
Low-affinity glucose transporter		*HXT1*	116 ± 6	82 ± 8	57 ± 2
High-affinity glucose transporter		*HXT2*	3329 ± 361	2133 ± 195	1585 ± 103
Low-affinity glucose transporter		*HXT3*	39 ± 10	39 ± 12	17 ± 5
High-affinity glucose transporter		*HXT4*	2273 ± 46	1046 ± 89	705 ± 89
Hexose transporter with moderate affinity for glucose, induced in the presence of non-fermentable carbon sources		*HXT5*	154 ± 25	153 ± 4	**346 ± 64**
Similarity to hexose transporter family members		*HXT16*	35 ± 4	**131 ± 26**	**172 ± 21**
Galactose permease		*GAL2*	13 ± 1	21 ± 8	**6125 ± 643**
Glycolysis					
Fructose-1,6-bisphosphatase	3	*FBP1*	14 ± 2	**37 ± 6**	**41 ± 2**
Glyceraldehyde-3-phosphate dehydrogenase	6	*TDH1*	1500 ± 145	1724 ± 71	820 ± 62
Glycerol metabolism					
Glycerol-3-phosphate dehydrogenase (cyt.)	11	*GPD1*	542 ± 35	**1228 ± 125**	**1126 ± 51**
Glycerol-3-phosphate dehydrogenase (mit.)		*GUT2*	181 ± 13	**393 ± 5**	**479 ± 35**
Glycerol kinase (cyt.)	12	*GUT1*	113 ± 2	160 ± 20	**229 ± 26**
Dihydroxyacetone kinase		*DAK2*	12 ± 0	**100 ± 15**	**167 ± 6**
Pentose phosphate pathway					
6-Phosphogluconate dehydrogenase	15	*GND2*	45 ± 3	**103 ± 17**	**118 ± 19**
Transketolase	18	*TKL2*	16 ± 3	**62 ± 15**	**87 ± 6**
Transaldolase	19	*YGR043C*	58 ± 10	**413 ± 47**	**557 ± 45**
Pyruvate branchpoint					
Alcohol dehydrogenase	21	*ADH2*	33 ± 5	**205 ± 47**	**333 ± 61**
Acetaldehyde dehydrogenase (NAD-dep., cyt.)	22	*ALD6*	576 ± 92	**1250 ± 179**	1015 ± 37
(NADP-dep., mit.)		*ALD4*	1286 ± 170	2366 ± 120	**3058 ± 173**
Acetyl CoA synthetase (non-mit.)		*ACS1*	307 ± 30	556 ± 97	**817 ± 9**
TCA and glyoxylate cycle					
Citrate synthase (mit.)	25	*CIT3*	19 ± 4	38 ± 4	**53 ± 8**
Isocitrate dehydrogenase (NAD-dep., mit.)	27	*IDH1*	192 ± 36	**517 ± 15**	**490 ± 106**
(NADP-dep., cyt.)		*IDP2*	24 ± 4	**57 ± 2**	**62 ± 8**
Succinate dehydrogenase (mit.)	28	*SDH1*	336 ± 11	569 ± 89	**940 ± 101**
		SDH3	705 ± 21	953 ± 132	**1500 ± 95**
Succinyl-coA ligase (mit.)		*LSC2*	278 ± 25	475 ± 87	**560 ± 22**
α-Ketoglutarate dehydrogenase (mit.)		*KGD1*	1156 ± 140	1856 ± 94	**2546 ± 178**
		KGD2	395 ± 33	694 ± 93	**961 ± 115**
Isocitrate lyase (cyt.)		*ICL1*	95 ± 4	**215 ± 26**	**252 ± 33**
Malate synthase (cyt.)		*MLS1*	20 ± 3	**43 ± 7**	**44 ± 9**
Galactose metabolism					
Galactokinase		*GAL1*	12 ± 0	13 ± 1	**3489 ± 181**
Galactose-1-phosphate uridyl transferase		*GAL7*	12 ± 0	12 ± 0	**2472 ± 126**
UDP-glucose-4-epimerase		*GAL10*	13 ± 1	14 ± 2	**3190 ± 423**
Transcriptional regulator involved in activation of the GAL genes in response to galactose		*GAL3*	42 ± 2	18 ± 4	**184 ± 8**
Phosphoglucomutase		*PGM2*	271 ± 23	337 ± 113	**794 ± 110**
Transcriptional regulator of GAL genes		*GAL80*	63 ± 4	35 ± 2	**133 ± 16**
Aldo-keto reductases					
Putative NADP(+) coupled glycerol dehydrogenase; member of the aldo-keto reductase family		*GCY1*	273 ± 26	173 ± 15	**1703 ± 172**
NADPH-dependent aldo-keto reductase		*YPR1*	146 ± 14	200 ± 10	**293 ± 6**
Regulatory proteins					
Negative regulator of the glucose-sensing signal transduction pathway		*MTH1*	770 ± 58	574 ± 23	**1220 ± 68**
Plasma membrane glucose receptor, serves as transmembrane glucose sensors generating an intracellular signal that induces expression of glucose transporter (HXT) genes		*RGT2*	67 ± 7	42 ± 3	29 ± 3
Transcription factor required for full Ty1 expression, Ty1-mediated gene activation, and haploid invasive and diploid pseudohyphal growth		*TEC1*	739 ± 38	314 ± 39	148 ± 21

[a] The numbers correspond to the enzymatic reactions in Fig. 1A.
[b] Significantly 2-fold up- and down regulated genes for a specific condition are indicated by boldface and underlined numbers, respectively.

Few significant differences were observed in other intracellular metabolite concentrations. The intracellular F1,6BP concentration was slightly lower in the IMS0002 strain under both growth conditions while the T6P concentration was higher, in particular during arabinose-limited growth (2.6 fold; Table 5). In lower glycolysis, the average pyruvate concentration was two-fold lower in strain IMS0002 during glucose-limited growth. Of the TCA intermediates, intracellular concentrations of malate and

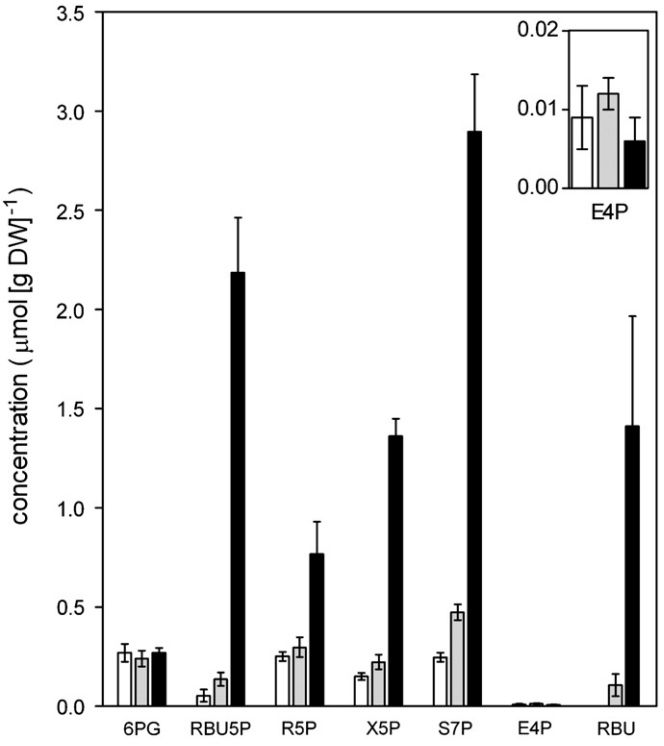

Fig. 4. Concentrations of 6-PG, the non-oxidative pentose phosphate pathway intermediates and RBU during anaerobic growth of: IMS0001, glucose-limited (white bar); IMS0002, glucose-limited (gray bar); and IMS0002, arabinose-limited (black bar). For IMS0002 growing on arabinose RBU5P represents the sum of D- and L-RBU5P. Data represent the average and standard deviation of three independent experiments. 6PG was determined by LC–MS. R5P, X5P, RBU5P, E4P, S7P and RBU were determined by a recently developed GC-IDMS method (Cipollina et al., 2009).

fumarate were about 2 times higher in strain IMS0002 during growth on glucose; intracellular citrate concentrations were about two-fold lower during growth on arabinose (Table 5).

3.5. Identification of possible rate-controlling reactions in arabinose metabolism

When concentrations of reactants and products of a reaction are known, the driving force for that specific reaction can be calculated from thermodynamic considerations. For the simple reaction A+B→C, the ratio Γ/K_{eq} can be calculated, in which Γ is the mass action ratio ([C]/([A]·[B]). At equilibrium, the net reaction rate is zero and $\Gamma/K_{eq}=1$, and hence the driving force of the reaction, defined as $1-\Gamma/K_{eq}$, is 0. For reactions with a high kinetic capacity, Γ/K_{eq} remains close to 1 at increasing rates while it decreases steeply when the kinetic capacity is low. Therefore, reactions with a high kinetic capacity show a nearly constant Γ/K_{eq} at increasing fluxes, while reactions with a low capacity display a strong decrease of Γ/K_{eq} and thus an increase in the driving force at increasing fluxes.

Mass action ratios and driving forces were calculated for the reactions of the non-oxidative PPP and for the reversible reactions of upper glycolysis by using the concentrations measured in this study and literature data for equilibrium constants (Table 6). Triosephosphate isomerase and phosphoglucose isomerase offered typical examples of near-equilibrium reactions. Despite the increased flux for arabinose-limited conditions, the mass action ratio for TPI remained constant in all three situations and close to the literature value for K_{eq} of 0.045, resulting in a driving

Table 5
Intra-cellular concentrations of glycolytic and TCA cycle intermediates during anaerobic glucose- and arabinose-limited chemostat cultures of *S. cerevisiae* strains IMS0002 and IMS0001 at a dilution rate of 0.03 h^{-1}. All data were obtained by LC-MS/MS analysis, except for GAP and DHAP which were measured by GC–MS (Cipollina et al., 2009). Data represent the average and standard deviation of three independent experiments.

strain	Carbon limitation	Metabolite concentration (μmol [g DW]$^{-1}$) ± SD															
		M6P	T6P	G1P	G6P	F6P	F1,6BP	GAP	DHAP	2PG/3PG	PEP	G3P	PYR	FUM	SUC	MAL	OXG	CIT
IMS0001	Glucose	0.99 ± 0.13	0.15 ± 0.09	0.57 ± 0.03	3.0 ± 0.2	0.53 ± 0.07	17.5 ± 2.6	0.05 ± 0.01	1.2 ± 0.2	0.46 ± 0.14	0.13 ± 0.06	0.48 ± 0.05	5.1 ± 1.4	0.54 ± 0.08	14.4 ± 0.9	2.4 ± 0.1	0.43 ± 0.04	10.2 ± 3.3
IMS0002	Glucose	1.3 ± 0.1	0.14 ± 0.06	0.54 ± 0.09	3.6 ± 0.1	0.64 ± 0.04	12.4 ± 2.2	0.06 ± 0.01	1.1 ± 0.2	0.37 ± 0.09	0.11 ± 0.05	0.56 ± 0.07	2.1 ± 0.3	0.91 ± 0.11	9.8 ± 1.1	5.0 ± 0.4	0.59 ± 0.07	10.4 ± 1.6
IMS0002	Arabinose	1.1 ± 0.1	0.42 ± 0.14	0.17 ± 0.05	2.7 ± 0.1	0.50 ± 0.04	10.1 ± 0.5	0.07 ± 0.02	1.5 ± 0.1	0.41 ± 0.05	0.10 ± 0.02	0.66 ± 0.05	4.4 ± 3.2	0.54 ± 0.1	9.0 ± 0.8	2.3 ± 0.3	0.50 ± 0.05	4.7 ± 1.0

Table 6
Thermodynamics of the reactions catalyzed by phosphoglucose isomerase (PGI), for fructose-1,6-bisphosphate aldolase (FBA), triosephosphate isomerase (TPI), transketolase (TK I and II), transaldolase (TAL), ribulose-5-phosphate epimerase (RPE) and ribulose-5-phosphate isomerase (RPI). The thermodynamics are determined for the strains and growth conditions analyzed in the present study: IMS0001, glucose-limited (IMS0001, glc); IMS0002, glucose-limited (IMS0002, glc); IMS0002, arabinose-limited (IMS0002, ara).

Enzyme	Reaction	K_{eq}	Reference	Γ[a]		
				IMS0001, Glc	IMS0002, Glc	IMS0002, Ara
PGI	G6P→F6P	0.28	Tewari et al. (1988)	0.18	0.18	0.18
FBA	FBP→GAP+DHAP	0.99×10^{-4} M	Veech et al. (1969)	1.48×10^{-6}	2.25×10^{-6}	4.07×10^{-6}
TPI	DHAP→GAP	0.045	Veech et al. (1969)	0.040	0.054	0.045
TK I[b]	R5P+X5P→GAP+S7P	2.08	Casazza and Veech (1986)	0.319	0.421	0.180
TAL	GAP+S7P→E4P+F6P	0.37	Casazza and Veech (1986)	0.394	0.275	0.016
TK II[b]	E4P+X5P→F6P+GAP	29.7	Casazza and Veech (1986)	19.11	14.11	3.98
RPE[c]	RBU5P→X5P	1.82	Casazza and Veech (1986)	2.85	1.63	Nd
RPI[c]	RBU5P→R5P	1.20	Casazza and Veech (1986)	4.74	2.18	Nd

[a] Γ is the mass action ratio, defined as the ratio between the product of all the molar product concentration divided by the product of all the molar reactant concentrations. For comparison of the mass action ratio of FBA with its K_{eq} value, the measured concentrations of FBP, GAP and DHAP were converted from μmol (g DW)$^{-1}$ into molar concentrations, assuming a cell volume of 2.3 ml (g DW)$^{-1}$ (Ditzelmüller et al., 1983).

[b] The transketolase I and II reactions refer to the same enzyme (i.e. transketolase).

[c] The GC–MS method used did not allow to distinguish between L- and D-ribulose-5-P. Since during growth on arabinose in IMS0002 both L- and D-ribulose-5-P are present, the mass action ratios of RPE and RPI could not be determined (Nd) for arabinose-limited growth. For the glucose-limited cultures of strains IMS0001 and IMS0002 it was assumed that no L-ribulose-5-P is present.

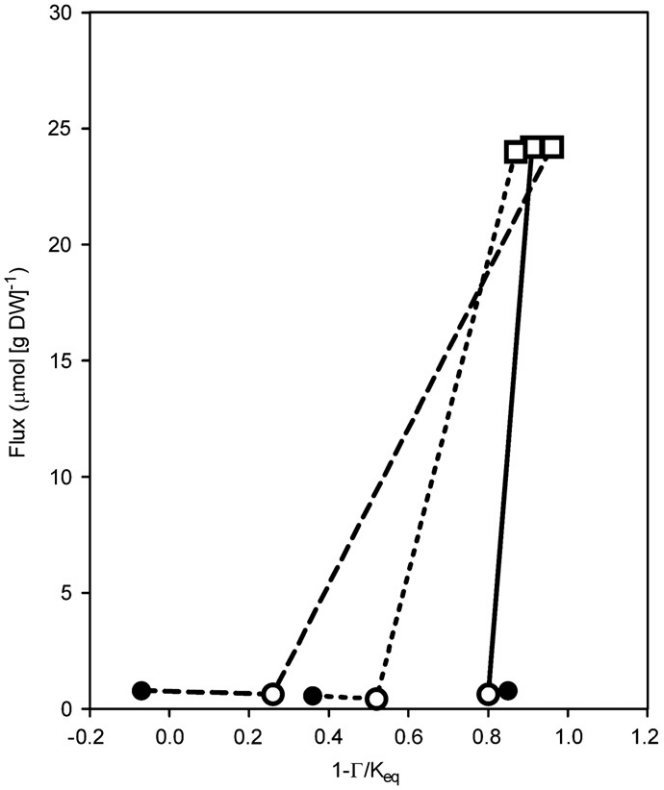

Fig. 5. Plot of fluxes, derived from the flux distribution model, versus driving forces ($1-\Gamma/K_{eq}$) of the reactions catalyzed by Transaldolase (striped line), Transketolase 1 (solid line) and Transketolase 2 (dotted line) under the conditions analyzed in the present study: IMS0001, glucose-limited (●); IMS0002, glucose-limited (○); IMS0002, arabinose-limited (□).

force close to 0. This indicates that this reaction is near equilibrium and that TPI has a high *in vivo* capacity. Although the direction and magnitude of the flux through PGI changed, its mass action ratio remained stable at around 0.18, suggesting that the reaction was close to equilibrium and that PGI had a high *in vivo* capacity, consistent with previous observations (Tewari et al., 1988). Clearly, the *in vivo* PGI K_{eq} of 0.18 is in contrast with the previously determined *in vitro* value of 0.28 (Tewari et al., 1988). Ribulose-5-phosphate epimerase and ribulose-5-phosphate isomerase are known to catalyze fast equilibrium reactions, similar to PGI and TPI (Selivanov et al., 2004; van Winden et al., 2002). Consequently, a mass action ratio close to equilibrium would be expected. However, the observed values for the mass action ratios of these two reactions differed for the different situations studied and from the literature values for their equilibrium constants. For fructose-1,6-bisphosphate aldolase, a weak relation between reaction rate and driving force was observed (not shown), suggesting a high *in vivo* capacity of this enzyme. The transketolase I reaction was close to equilibrium in all three conditions. The drastically increased flux at a constant driving force indicates that also this reaction has a high capacity (Fig. 5).

In contrast to the observations for transketolase reaction I, major changes in both flux and driving force were observed for transaldolase and transketolase reaction II. Interestingly, although under glucose-limited conditions the flux through transaldolase and the transketolase reaction II did not change between IMS0001 and IMS0002, the driving force increased for IMS0002, suggesting kinetic differences for transketolase reaction II in strains IMS0001 and IMS0002 (Fig. 5). When growing on arabinose, the 34-fold increase of the flux through transaldolase coincided with a decrease of the mass action ratio from close to the equilibrium value of 0.37 in glucose-limited cultures to a 23-fold lower value of 0.016 in the arabinose-limited cultures (Table 6), thereby drastically increasing the driving force of the reaction. Although the difference of the mass action ratio of the transketolase reaction II was less pronounced (Table 6), its almost 5-fold lower value in arabinose-limited cultures relative to that in glucose-limited cultures still reflects the impact of the 34-fold higher flux during growth on arabinose. Taken together, these data suggest that transaldolase and transketolase reaction II may exert a high degree of control on arabinose fermentation in strain IMS0002.

3.6. *TKL2 and YGR043C (TAL2) contribute to arabinose utilization in strain IMS0002*

The combination of the identification of transaldolase and transketolase as possible rate-controlling steps in arabinose utilization and the up-regulation of the transcript levels of *TKL2* and *YGR043C*, encoding 'minor' isoenzymes of transaldolase and transketolase,

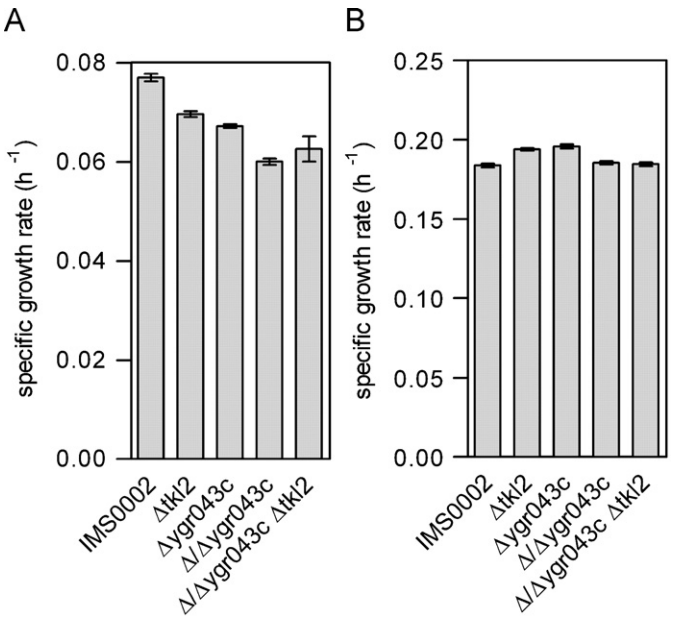

Fig. 6. Specific growth rates (μ) of strain IMS0002 and the deletion strains IMS0013 (Δ*ygr043c*), IMS0014 (Δ*tkl2*), IMS0020 (Δ/Δ*ygr043c*) and IMS0022 (Δ/Δ*ygr043c* Δ*tkl2*), grown anaerobically in sequential batches in MY containing 20 g l^{-1} of arabinose (A) or glucose (B). For each strain, five batches were repeated (in duplo for arabinose), of which the final three were used to determine the specific growth rate based on the carbon-dioxide production profile. The average specific growth rate of the three batches was considered as representative for the strain.

suggests a role of these two genes in arabinose utilization by IMS0002. To investigate their involvement, which was surprising in view of the overexpression of *TAL1* and *TKL1* in the IMS0001 strain (Kuyper et al., 2005a, 2005b), deletion mutants in *YGR043C* and *TKL2* were constructed in strain IMS0002 (Table 1). As indicated above, a 250 kb fragment of chromosome VII was probably duplicated during the evolution of IMS0002, contributing to upregulation of the transcripts of *YGR043C* and approximately 60 other genes (Fig. 3). Indeed, diagnostic PCR during construction of the Δ*ygr043c* strain confirmed the presence of two copies of this gene in IMS0002. Hence, also a double *ygr043c* knockout strain was constructed (Δ/Δ*ygr043c*).

To examine the effect of the deletions of *TKL2* and *YGR043C*, the growth rates of the deletion strains were determined during anaerobic growth on arabinose. To increase the reproducibility and minimize effects of precultivation (Abbott et al., 2009), each strain was cultivated anaerobically in five sequential batches in MYA and for each single batch cultivation the specific growth rate was determined from the carbon-dioxide production profile. The specific growth rates in the first two batch cultures consistently showed an increase, therefore the average specific growth rate calculated from final three cultures were used to compare the different strains. The specific growth rate during anaerobic growth on arabinose (μ_{ara}) was significantly lower (p-value < 0.05) in each of the deletion strains than in strain IMS0002 (Fig. 6). The single *ygr043c* (IMS0013) and *tkl2* knockout strains showed growth rate reductions of 13% and 10%, respectively. The most pronounced reduction was observed for the Δ/Δ*ygr043c* strain (IMS0020), exhibiting an average μ_{ara} of $0.061 \pm 0.002\ h^{-1}$, which is 79% of that of strain IMS0002 ($0.077 \pm 0.002\ h^{-1}$). Subsequent deletion of *TKL2* in the Δ/Δ*ygr043c* strain however, did not result in a further significant change of μ_{ara} (0.063 ± 0.006). As a reference, the strains were also grown for five sequential batches in MYG. Compared to IMS0002, deletion of *YGR043C* or *TKL2* did not result in lower specific growth rates during growth on glucose (μ_{glc}), indicating that the observed effect on the specific growth rate are specific for growth on arabinose. The presence of a *KanMX* marker did not negatively affect the specific growth rate on glucose, as also supported by the identical μ_{ara} of strain IMS0013 and its marker-free descendant strain IMS0019 (data not shown).

3.7. Gal2 is responsible for arabinose transport in strain IMS0002

Gal2p, the *S. cerevisiae* galactose permease, is capable of importing arabinose (Kou et al., 1970), and *GAL2* overexpression has been shown to result in improved arabinose uptake (Becker and Boles, 2003). Although other hexose transporter genes showed increased transcript levels in strain IMS0002 (*HXT16*) or in the presence of arabinose (*HXT5*), the strongly increased transcript levels of *GAL2* in arabinose-grown cultures (Table 4) suggested it plays a dominant role in arabinose transport in strain IMS0002. To test this hypothesis, an IMS0002 Δ*gal2* strain (IMS0012) was constructed, and tested for growth on arabinose as sole carbon source by cultivation in MYA in a shake flask at 30 °C. Even after 350 h of incubation in MYA, neither growth nor consumption of arabinose was observed (data not shown), thus demonstrating that Gal2p is essential for arabinose transport in IMS0002.

4. Discussion

4.1. Pentose transport and the GAL regulon

When evolutionary engineering is applied to improve the fermentation kinetics for the non-native substrates xylose and arabinose, it is not surprising that changes occur at the level of transport. In previous research, transcriptome analysis of the evolutionary engineered xylose-isomerase-based xylose-fermenting strain RWB218 revealed increased transcript levels of the hexose transporter genes *HXT1* and *HXT4* (van Maris et al., 2007), of which *HXT4* was previously shown to transport xylose (Hamacher et al., 2002). Similar to what was observed for two XR/XDH-based xylose-utilizing *S. cerevisiae* strains (Sonderegger et al., 2004; Wahlbom et al., 2003), increased transcript levels of *HXT5* and *HXT16* observed for arabinose-limited growth of IMS0002 (Table 4) might suggest a role of these hexose transporters in arabinose transport. The strong up-regulation of *GAL2* in arabinose-grown cultures of strain IMS0002 however, strongly points towards the involvement of galactose permease (Gal2p)(Becker and Boles, 2003; Hamacher et al., 2002; Kou et al., 1970). Indeed, deletion of *GAL2,* which is known to transport arabinose (Becker and Boles, 2003; Kou et al., 1970) and xylose (Hamacher et al., 2002), completely abolished the ability of IMS0002 to grow on arabinose. Apparently, the changed transcript levels of other *HXT* genes in this strain do not reflect their active involvement in arabinose import.

The changes in *GAL2*, *GAL1*, *GAL7* and *GAL10* expression in arabinose-limited cultures of strain IMS0002, was previously also observed for several xylose-utilizing *S. cerevisiae* strains (Bengtsson et al., 2008; Sonderegger et al., 2004; Wahlbom et al., 2003). Increased transcript levels of the GAL-regulon in IMS0002 required the presence of arabinose, suggesting that arabinose based induction occurred via Gal3p, similar to galactose-induced expression (Platt and Reece, 1998). Contamination of L-arabinose with galactose as an explanation for induction of the GAL genes, was excluded by HPLC analysis of concentrated solutions of the arabinose used in the growth experiments. In addition, anaerobic carbon-limited chemostat cultivation of the congenic reference strain CEN.PK 113-7D on a mixture of 10 g l^{-1} glucose and 10 g l^{-1} L-arabinose did not result in induction of the GAL regulon,

while growth on a mixture of 10 g l^{-1} glucose and 10 g l^{-1} galactose did (results not shown). This confirmed the absence of galactose in the arabinose and demonstrated that induction of the *GAL* genes by arabinose is an acquired trait of the evolved strain IMS0002. We hypothesized that mutations in the *GAL3* gene (encoding the regulator Gal3p) or in *GAL2* itself might explain arabinose induction. However, DNA sequence analysis of *GAL3* and *GAL1* (which, like Gal3p, can act as a positive regulator of *GAL* genes (Bhat and Hopper, 1992)), *GAL2,* and their upstream non-coding regions in strain IMS0002 did not reveal any mutations when compared to strain IMS0001 (results not shown). Hence, the mechanism by which arabinose induces the GAL regulon in strain IMS0002 remains to be identified.

4.2. Reconfiguring the pentose-phosphate pathway for a catabolic role

Growth of engineered *S. cerevisiae* strains on pentoses causes a drastic change in the role of the PPP. During anaerobic glucose-limited growth glycolysis was the major catabolic pathway from sugar to F6P and triose phosphates. In contrast, the non-oxidative part of the PPP fulfilled this key catabolic role in arabinose-limited cultures. Similar to xylose-consuming *S. cerevisiae* strains (Kötter and Ciriacy, 1993; Pitkänen et al., 2005; Zaldivar et al., 2002), elevated intracellular metabolite concentrations of S7P and X5P in IMS0002 under arabinose-limited conditions suggested kinetic constraints in the PPP, in particular for the transaldolase and transketolase II reactions (Table 6 and Fig. 5). It can be argued if the increased concentrations merely reflects a high flux. In contrast, in the naturally xylose-fermenting yeast *Pichia stipitis* (recently renamed to *Scheffersomyces stipitis* (Kurtzman and Suzuki, 2010)) intracellular concentrations of non-oxidative PPP intermediates do not substantially differ between in glucose- and xylose-grown cultures (Kötter and Ciriacy, 1993).

Further support for the hypothesis that transaldolase and transketolase had a strong influence on rates of arabinose fermentation was provided by increased expression of *TKL2* and the increased expression and gene duplication of *YGR043C* in the evolved strain IMS0002. Deletion of *TKL2* and of both copies of *YGR043C* resulted in significantly lower specific growth rates on arabinose (Fig. 6). Since both *TAL1* and *TKL1* are strongly overexpressed (Kuyper et al., 2005a, 2005b), this raises the question how these two isozymes support the already high activities of transaldolase and transketolase (Kuyper et al., 2005a, 2005b). Deletion of *TKL2* did not result in a significant decrease of transketolase I activity (results not shown). This however, does not exclude an important *in vivo* role of Tkl2p in transketolase reaction II, for which a significant deviation from equilibrium was demonstrated in the evolved strain. Similarly, although no significant contribution of Ygr043p (Tal2p) was established when transaldolase activity was assayed in the non-physiological direction (E4P+F6P→S7P+G3P), a stronger contribution to the reverese reaction cannot be excluded. Alternatively, Tkl2p and Tal2p may differ in substrate specificity or affinity from their better studied 'major' isoenzymes Tkl1p and Tal1p, or might even catalyze unconventional transketolase and transaldolase (half)-reactions (Kleijn et al., 2005; van Winden et al., 2001).

Although no direct indications for kinetic constraints in glycolysis were found, higher T6P and lower F1,6BP levels observed during growth on arabinose, compared to glucose may negatively affect glycolytic flux through T6P and F1,6BP mediated metabolic control. These metabolites, together with adenine nucleotides and F2,6BP, play a crucial role in fine tuning the glycolytic flux through their roles as allosteric activator of pyruvate kinase and inhibitor of hexokinase activity (Boles et al., 1997; Gancedo and Flores, 2004; Goncalves and Planta, 1998). In addition the absence of a flux through hexokinase, a protein involved in the signaling network promoting glucose-mediated catabolite repression and growth (Ahuatzi et al., 2007; Ashe et al., 2000; Westergaard et al., 2007), might influence flux regulation as well as the altered transcript levels of many genes whose expression is affected by glucose catabolite repression.

4.3. Chemostat-based multilevel analysis in metabolic engineering

By comparing the two strains in chemostat cultures, bias due to growth-rate differences that originate from the strain background or variation in the carbon source was eliminated. The macroscopic fluxes, the concentrations of glycolytic and TCA cycle intermediates, amino acids and adenine nucleotides showed a limited number of differences between the two strains that were mostly focussed around the pentose-phosphate pathway. Despite this highly reproducible experimental set-up, pair-wise analysis of genome-wide transcript levels did reveal numerous strain-specific differences (Fig. 2; Cluster I, III and IV), suggesting that the genetic background of the two strains are quite different. Not only does the relevance of up- or down regulation for the majority of these genes remain unclear, but this study alone already identified two sources of background mutations that are likely to not be involved in the selected phenotype: (i) It is likely that only one (*YGR043C*) or a few of the genes in the duplicated 250 kb area on chromosome VII contribute to the phenotype of strain IMS0002. The upregulation of the majority of these genes is likely to be collateral damage. (ii) Along with the crucial upregulation of the Gal2p 'arabinose' transporter in IMS0002 other genes of the Gal-operon were upregulated. Although once such duplications have been established they can be taken into account in the data analysis, these examples underline the benefit of analyzing multiple, in parallel evolved strains to facilitate differentiation between background and phenotype-relevant mutations that are involved in pentose utilization.

Overall, the results shown in this study support the view that in *S. cerevisiae* the PPP has not evolved as a catabolic pathway. Although the accumulation of sugar phosphates in the PPP suggest kinetic constraints in this pathway, it has been reported that *S. cerevisiae* can grow anaerobically on xylose at higher rates than the μ_{max} of IMS0002 on arabinose (Kuyper et al., 2005b). It therefore seems reasonable to anticipate further improvements in the rates of arabinose fermentation.

Acknowledgments

This project was financially supported by the Netherlands Ministry of Economic Affairs and the B-Basic partner organizations (www.b-basic.nl) through B-Basic, a public-private NWO-ACTS program (ACTS=Advanced Chemical Technologies for Sustainability). The Kluyver Centre for Genomics of Industrial Fermentation is supported by the Netherlands Genomics Initiative. We thank Marjan de Mey for providing L-ribulose, Jean-Marc Daran for assisting in the transcript analysis, and Marinka Almering, Ward Blanken, Max Clabbers and Angela ten Pierick for technical assistance.

Appendix A. Supplementary material

Supplementary data associated with this article can be found in the online version at doi:10.1016/j.ymben.2010.08.003.

References

Abbott, D.A., Suir, E., Duong, G.H., de Hulster, E., Pronk, J.T., van Maris, A.J.A., 2009. Catalase overexpression reduces lactic acid-induced oxidative stress in *Saccharomyces cerevisiae*. Appl. Environ. Microbiol. 75, 2320–2325.

Ahuatzi, D., Riera, A., Pelaez, R., Herrero, P., Moreno, F., 2007. Hxk2 regulates the phosphorylation state of Mig1 and therefore its nucleocytoplasmic distribution. J. Biol. Chem. 282, 4485–4493.

Andreasen, A.A., Stier, T.J., 1953. Anaerobic nutrition of *Saccharomyces cerevisiae*. I. Ergosterol requirement for growth in a defined medium. J. Cell Physiol. 41, 23–36.

Andreasen, A.A., Stier, T.J., 1954. Anaerobic nutrition of *Saccharomyces cerevisiae*. II. Unsaturated fatty acid requirement for growth in a defined medium. J. Cell Physiol. 43, 271–281.

Aristidou, A., Penttilä, M., 2000. Metabolic engineering applications to renewable resource utilization. Curr. Opin. Biotechnol. 11, 187–198.

Ashe, M.P., De Long, S.K., Sachs, A.B., 2000. Glucose depletion rapidly inhibits translation initiation in yeast. Mol. Biol. Cell 11, 833–848.

Atkinson, D.E., 1968. Energy charge of adenylate pool as a regulatory parameter. Interaction with feedback modifiers. Biochemistry 7, 4030–4034.

Becker, J., Boles, E., 2003. A modified *Saccharomyces cerevisiae* strain that consumes L-arabinose and produces ethanol. Appl. Environ. Microbiol. 69, 4144–4150.

Bengtsson, O., Jeppsson, M., Sonderegger, M., Parachin, N.S., Sauer, U., Hahn-Hägerdal, B., Gorwa-Grauslund, M.F., 2008. Identification of common traits in improved xylose-growing *Saccharomyces cerevisiae* for inverse metabolic engineering. Yeast 25, 835–847.

Bera, A.K., Sedlak, M., Khan, A., Ho, N.W., 2010. Establishment of L-arabinose fermentation in glucose/xylose co-fermenting recombinant *Saccharomyces cerevisiae* 424A(LNH-ST) by genetic engineering. Appl. Microbiol. Biotechnol.

Bettiga, M., Bengtsson, O., Hahn-Hägerdal, B., Gorwa-Grauslund, M.F., 2009. Arabinose and xylose fermentation by recombinant *Saccharomyces cerevisiae* expressing a fungal pentose utilization pathway. Microb. Cell Fact. 8, 40.

Bhat, P.J., Hopper, J.E., 1992. Overproduction of the Gal1 or Gal3 protein causes galactose-independent activation of the Gal4 protein—evidence for a new model of induction for the yeast Gal Mel regulon. Mol. Cell. Biol. 12, 2701–2707.

Boer, V.M., de Winde, J.H., Pronk, J.T., Piper, M.D., 2003. The genome-wide transcriptional responses of *Saccharomyces cerevisiae* grown on glucose in aerobic chemostat cultures limited for carbon, nitrogen, phosphorus, or sulfur. J. Biol. Chem. 278, 3265–3274.

Boles, E., Schulte, F., Miosga, T., Freidel, K., Schlüter, E., Zimmermann, F.K., Hollenberg, C.P., Heinisch, J.J., 1997. Characterization of a glucose-repressed pyruvate kinase (Pyk2p) in *Saccharomyces cerevisiae* that is catalytically insensitive to fructose-1,6-bisphosphate. J. Bacteriol. 179, 2987–2993.

Casazza, J.P., Veech, R.L., 1986. The interdependence of glycolytic and pentose cycle intermediates in ad libitum fed rats. J. Biol. Chem. 261, 690–698.

Cipollina, C., ten Pierick, A., Canelas, A., Seifar, R.M., van Maris, A.J.A., Van Dam, J.C., Heijnen, J.J., 2009. A comprehensive method for the quantification of the non-oxidative pentose phosphate pathway intermediates in *Saccharomyces cerevisiae* by GC-IDMS. J. Chromatogr. B 877, 3231–3236.

Daran-Lapujade, P., Daran, J.M., van Maris, A.J.A., de Winde, J.H., Pronk, J.T., 2009. Chemostat-based micro-array analysis in baker's yeast. Adv. Microb. Physiol. 54, 257–311.

Daran-Lapujade, P., Jansen, M.L., Daran, J.M., van Gulik, W., de Winde, J.H., Pronk, J.T., 2004. Role of transcriptional regulation in controlling fluxes in central carbon metabolism of *Saccharomyces cerevisiae*. A chemostat culture study. J. Biol. Chem. 279, 9125–9138.

Ditzelmüller, G., Wöhrer, W., Kubicek, C.P., Röhr, M., 1983. Nucleotide pools of growing, synchronized and stressed cultures of *Saccharomyces cerevisiae*. Arch. Microbiol. 135, 63–67.

Enomoto, K., Arikawa, Y., Muratsubaki, H., 2002. Physiological role of soluble fumarate reductase in redox balancing during anaerobiosis in *Saccharomyces cerevisiae*. FEMS Microbiol. Lett. 215, 103–108.

Fernandes, L., Rodrigues-Pousada, C., Struhl, K., 1997. Yap, a novel family of eight bZIP proteins in *Saccharomyces cerevisiae* with distinct biological functions. Mol. Cell Biol. 17, 6982–6993.

Gancedo, C., Flores, C.L., 2004. The importance of a functional trehalose biosynthetic pathway for the life of yeasts and fungi. FEMS Yeast Res. 4, 351–359.

Gietz, R.D., Woods, R.A., 2002. Transformation of yeast by lithium acetate/single-stranded carrier DNA/polyethylene glycol method. Methods Enzymol. 350, 87–96.

Goncalves, P., Planta, R.J., 1998. Starting up yeast glycolysis. Trends Microbiol. 6, 314–319.

Güldener, U., Heck, S., Fiedler, T., Beinhauer, J., Hegemann, J.H., 1996. A new efficient gene disruption cassette for repeated use in budding yeast. Nucleic Acids Res. 24, 2519–2524.

Güldener, U., Heinisch, J., Koehler, G.J., Voss, D., Hegemann, J.H., 2002. A second set of loxP marker cassettes for Cre-mediated multiple gene knockouts in budding yeast. Nucleic Acids Res. 30, e23.

Hahn-Hägerdal, B., Karhumaa, K., Jeppsson, M., Gorwa-Grauslund, M.F., 2007. Metabolic engineering for pentose utilization in *Saccharomyces cerevisiae*. Adv. Biochem. Eng. Biotechnol. 108, 147–177.

Hamacher, T., Becker, J., Gardonyi, M., Hahn-Hägerdal, B., Boles, E., 2002. Characterization of the xylose-transporting properties of yeast hexose transporters and their influence on xylose utilization. Microbiology 148, 2783–2788.

Harbison, C.T., Gordon, D.B., Lee, T.I., Rinaldi, N.J., Macisaac, K.D., Danford, T.W., Hannett, N.M., Tagne, J.B., Reynolds, D.B., Yoo, J., Jennings, E.G., Zeitlinger, J., Pokholok, D.K., Kellis, M., Rolfe, P.A., Takusagawa, K.T., Lander, E.S., Gifford, D.K., Fraenkel, E., Young, R.A., 2004. Transcriptional regulatory code of a eukaryotic genome. Nature 431, 99–104.

Huang, H., Rong, H., Li, X., Tong, S., Zhu, Z., Niu, L., Teng, M., 2008. The crystal structure and identification of NQM1/YGR043C, a transaldolase from *Saccharomyces cerevisiae*. Proteins 73, 1076–1081.

Jeffries, T.W., Jin, Y.S., 2004. Metabolic engineering for improved fermentation of pentoses by yeasts. Appl. Microbiol. Biotechnol. 63, 495–509.

Jeppsson, M., Johansson, B., Hahn-Hägerdal, B., Gorwa-Grauslund, M.F., 2002. Reduced oxidative pentose phosphate pathway flux in recombinant xylose-utilizing *Saccharomyces cerevisiae* strains improves the ethanol yield from xylose. Appl. Environ. Microbiol. 68, 1604–1609.

Jin, Y.S., Laplaza, J.M., Jeffries, T.W., 2004. *Saccharomyces cerevisiae* engineered for xylose metabolism exhibits a respiratory response. Appl. Environ. Microbiol. 70, 6816–6825.

Kleijn, R.J., van Winden, W.A., van Gulik, W.M., Heijnen, J.J., 2005. Revisiting the ^{13}C-label distribution of the non-oxidative branch of the pentose phosphate pathway based upon kinetic and genetic evidence. FEBS J. 272, 4970–4982.

Knijnenburg, T.A., de Winde, J.H., Daran, J.M., Daran-Lapujade, P., Pronk, J.T., Reinders, M.J.T., Wessels, L.F.A., 2007. Exploiting combinatorial cultivation conditions to infer transcriptional regulation. BMC Genomics, 8.

Kötter, P., Ciriacy, M., 1993. Xylose fermentation by *Saccharomyces cerevisiae*. Appl. Microbiol. Biotechnol. 38, 776–783.

Kou, S.C., Christensen, M.S., Cirillo, V.P., 1970. Galactose transport in *Saccharomyces cerevisiae* II. Characteristics of galactose uptake and exchange in galactokinaseless cells. J. Bacteriol. 103, 671–678.

Kurtzman, C.P., Suzuki, M., 2010. Phylogenetic analysis of ascomycete yeasts that form coenzyme Q-9 and the proposal of the new genera *Babjeviella*, *Meyerozyma*, *Millerozyma*, *Priceomyces*, and *Scheffersomyces*. Mycoscience 51, 2–14.

Kuyper, M., Hartog, M.M., Toirkens, M.J., Almering, M.J., Winkler, A.A., van Dijken, J.P., Pronk, J.T., 2005a. Metabolic engineering of a xylose-isomerase-expressing *Saccharomyces cerevisiae* strain for rapid anaerobic xylose fermentation. FEMS Yeast Res. 5, 399–409.

Kuyper, M., Toirkens, M.J., Diderich, J.A., Winkler, A.A., van Dijken, J.P., Pronk, J.T., 2005b. Evolutionary engineering of mixed-sugar utilization by a xylose-fermenting *Saccharomyces cerevisiae* strain. FEMS Yeast Res. 5, 925–934.

Lange, H.C., 2002. Quantitative physiology of *S. cerevisiae* using metabolic network analysis. Ph.D. Thesis, Delft University of Technology, Department of Biotechnology, the Netherlands.

Mashego, M.R., Wu, L., Van Dam, J.C., Ras, C., Vinke, J.L., van Winden, W.A., van Gulik, W.M., Heijnen, J.J., 2004. MIRACLE: mass isotopomer ratio analysis of U–^{13}C-labeled extracts. A new method for accurate quantification of changes in concentrations of intracellular metabolites. Biotechnol. Bioeng. 85, 620–628.

Nasution, U., van Gulik, W.M., Ras, C., Proell, A., Heijnen, J.J., 2008. A metabolome study of the steady-state relation between central metabolism, amino acid biosynthesis and penicillin production in *Penicillium chrysogenum*. Metab. Eng. 10, 10–23.

Nissen, T.L., Schulze, U., Nielsen, J., Villadsen, J., 1997. Flux distributions in anaerobic, glucose-limited continuous cultures of *Saccharomyces cerevisiae*. Microbiology 143, 203–218.

Norbeck, J., Blomberg, A., 1997. Metabolic and regulatory changes associated with growth of *Saccharomyces cerevisiae* in 1.4 m NaCl—evidence for osmotic induction of glycerol dissimilation via the dihydroxyacetone pathway. J. Biol. Chem. 272, 5544–5554.

Piper, M.D.W., Daran-Lapujade, P., Bro, C., Regenberg, B., Knudsen, S., Nielsen, J., Pronk, J.T., 2002. Reproducibility of oligonucleotide microarray transcriptome analyses. An interlaboratory comparison using chemostat cultures of *Saccharomyces cerevisiae*. J. Biol. Chem. 277, 37001–37008.

Pitkänen, J.P., Aristidou, A., Salusjärvi, L., Ruohonen, L., Penttilä, M., 2003. Metabolic flux analysis of xylose metabolism in recombinant *Saccharomyces cerevisiae* using continuous culture. Metab. Eng. 5, 16–31.

Pitkänen, J.P., Rintala, E., Aristidou, A., Ruohonen, L., Penttilä, M., 2005. Xylose chemostat isolates of *Saccharomyces cerevisiae* show altered metabolite and enzyme levels compared with xylose, glucose, and ethanol metabolism of the original strain. Appl. Microbiol. Biotechnol. 67, 827–837.

Platt, A., Reece, R.J., 1998. The yeast galactose genetic switch is mediated by the formation of a Gal4p–Gal80p–Gal3p complex. EMBO J. 17, 4086–4091.

Richard, P., Verho, R., Putkonen, M., Londesborough, J., Penttilä, M., 2003. Production of ethanol from L-arabinose by *Saccharomyces cerevisiae* containing a fungal L-arabinose pathway. FEMS Yeast Res. 3, 185–189.

Runquist, D., Hahn-Hägerdal, B., Bettiga, M., 2009. Increased expression of the oxidative pentose phosphate pathway and gluconeogenesis in anaerobically growing xylose-utilizing *Saccharomyces cerevisiae*. Microb. Cell Fact., 8.

Salusjärvi, L., Pitkänen, J.P., Aristidou, A., Ruohonen, L., Penttilä, M., 2006. Transcription analysis of recombinant *Saccharomyces cerevisiae* reveals novel responses to xylose. Appl. Biochem. Biotechnol. 128, 237–274.

Schaaff-Gerstenschläger, I., Mannhaupt, G., Vetter, I., Zimmermann, F.K., Feldmann, H., 1993. *Tkl2*, a second transketolase gene of *Saccharomyces cerevisiae*—cloning, sequence and deletion analysis of the gene. Eur. J. Biochem. 217, 487–492.

Sedlak, M., Ho, N.W., 2004. Production of ethanol from cellulosic biomass hydrolysates using genetically engineered *Saccharomyces* yeast capable of cofermenting glucose and xylose. Appl. Biochem. Biotechnol. 113–116, 403–416.

Sedlak, M., Ho, N.W.Y., 2001. Expression of *E. coli araBAD* operon encoding enzymes for metabolizing L-arabinose in *Saccharomyces cerevisiae*. Enzyme Microb. Technol. 28, 16–24.

Seifar, R.M., Ras, C., Van Dam, J.C., van Gulik, W.M., Heijnen, J.J., van Winden, W.A., 2009. Simultaneous quantification of free nucleotides in complex biological samples using ion pair reversed phase liquid chromatography isotope dilution tandem mass spectrometry. Anal. Biochem. 388, 213–219.

Selivanov, V.A., Puigjaner, J., Sillero, A., Centelles, J.J., Ramos-Montoya, A., Lee, P.W., Cascante, M., 2004. An optimized algorithm for flux estimation from isotopomer distribution in glucose metabolites. Bioinformatics 20, 3387–3397.

Sonderegger, M., Jeppsson, M., Hahn-Hägerdal, B., Sauer, U., 2004. Molecular basis for anaerobic growth of *Saccharomyces cerevisiae* on xylose, investigated by global gene expression and metabolic flux analysis. Appl. Environ. Microbiol. 70, 2307–2317.

Sonderegger, M., Sauer, U., 2003. Evolutionary engineering of *Saccharomyces cerevisiae* for anaerobic growth on xylose. Appl. Environ. Microbiol. 69, 1990–1998.

Tewari, Y.B., Steckler, D.K., Goldberg, R.N., 1988. Thermodynamics of isomerization reactions involving sugar phosphates. J. Biol. Chem. 263, 3664–3669.

Vallino, J.J., Stephanopoulos, G., 1990. Flux determinations in cellular bioreaction networks: applications to lysine fermentations. In: S.K. Skidar, M. Bier, P. Todd (Eds.), Frontiers in Bioprocess. CRC Press, Boca Raton, FL, pp. 205–219.

Van Dam, J.C., Eman, M.R., Frank, J., Lange, H.C., van Dedem, G.W.K., Heijnen, J.J., 2002. Analysis of glycolytic metabolites in *Saccharomyces cerevisiae* using anion exchange chromatography and electrospray ionization with tandem mass spectrometric detection. Anal. Chim. Acta 460, 209–218.

van Dijken, J.P., Scheffers, W.A., 1986. Redox balances in the metabolism of sugars by yeasts. FEMS Microbiol. Rev. 32, 199–224.

van Gulik, W.M., Heijnen, J.J., 1995. A metabolic network stoichiometry analysis of microbial growth and product formation. Biotechnol. Bioeng. 48, 681–698.

van Maris, A.J.A., Winkler, A.A., Kuyper, M., de Laat, W.T., van Dijken, J.P., Pronk, J.T., 2007. Development of efficient xylose fermentation in *Saccharomyces cerevisiae*: xylose isomerase as a key component. Adv. Biochem. Eng. Biotechnol. 108, 179–204.

van Urk, H., Mak, P.R., Scheffers, W.A., van Dijken, J.P., 1988. Metabolic responses of *Saccharomyces cerevisiae* CBS 8066 and *Candida utilis* CBS 621 upon transition from glucose limitation to glucose excess. Yeast 4, 283–291.

van Winden, W., Verheijen, P., Heijnen, S., 2001. Possible pitfalls of flux calculations based on ^{13}C-labeling. Metab. Eng. 3, 151–162.

van Winden, W.A., Heijnen, J.J., Verheijen, P.J., 2002. Cumulative bondomers: a new concept in flux analysis from 2D [^{13}C,^{1}H] COSY NMR data. Biotechnol. Bioeng. 80, 731–745.

Veech, R.L., Raijman, L., Dalziel, K., Krebs, H.A., 1969. Disequilibrium in triose phosphate isomerase system in rat liver. Biochem. J. 115, 837–842.

Verduyn, C., Postma, E., Scheffers, W.A., van Dijken, J.P., 1990. Physiology of *Saccharomyces cerevisiae* in anaerobic glucose-limited chemostat cultures. J. Gen. Microbiol. 136, 395–403.

Verduyn, C., Postma, E., Scheffers, W.A., van Dijken, J.P., 1992. Effect of benzoic acid on metabolic fluxes in yeasts: a continuous-culture study on the regulation of respiration and alcoholic fermentation. Yeast 8, 501–517.

Wahlbom, C.F., Cordero Otero, R.R., van Zyl, W.H., Hahn-Hägerdal, B., Jonsson, L.J., 2003. Molecular analysis of a *Saccharomyces cerevisiae* mutant with improved ability to utilize xylose shows enhanced expression of proteins involved in transport, initial xylose metabolism, and the pentose phosphate pathway. Appl. Environ. Microbiol. 69, 740–746.

Wahlbom, C.F., Eliasson, A., Hahn-Hägerdal, B., 2001. Intracellular fluxes in a recombinant xylose-utilizing *Saccharomyces cerevisiae* cultivated anaerobically at different dilution rates and feed concentrations. Biotechnol. Bioeng. 72, 289–296.

Ward, M.P., Gimeno, C.J., Fink, G.R., Garrett, S., 1995. SOK2 may regulate cyclic AMP-dependent protein kinase-stimulated growth and pseudohyphal development by repressing transcription. Mol. Cell Biol. 15, 6854–6863.

Westergaard, S.L., Oliveira, A.P., Bro, C., Olsson, L., Nielsen, J., 2007. A systems biology approach to study glucose repression in the yeast *Saccharomyces cerevisiae*. Biotechnol. Bioeng. 96, 134–145.

Weusthuis, R.A., Visser, W., Pronk, J.T., Scheffers, W.A., van Dijken, J.P., 1994. Effects of oxygen limitation on sugar metabolism in yeasts—a continuous-culture study of the Kluyver effect. Microbiology 140, 703–715.

Wisselink, H.W., Toirkens, M.J., del Rosario Franco, B.M., Winkler, A.A., van Dijken, J.P., Pronk, J.T., van Maris, A.J.A., 2007. Engineering of *Saccharomyces cerevisiae* for efficient anaerobic alcoholic fermentation of L-arabinose. Appl. Environ. Microbiol. 73, 4881–4891.

Wu, L., Mashego, M.R., Van Dam, J.C., Proell, A.M., Vinke, J.L., Ras, C., van Winden, W.A., van Gulik, W.M., Heijnen, J.J., 2005. Quantitative analysis of the microbial metabolome by isotope dilution mass spectrometry using uniformly ^{13}C-labeled cell extracts as internal standards. Anal. Biochem. 336, 164–171.

Zaldivar, J., Borges, A., Johansson, B., Smits, H.P., Villas-Boas, S.G., Nielsen, J., Olsson, L., 2002. Fermentation performance and intracellular metabolite patterns in laboratory and industrial xylose-fermenting *Saccharomyces cerevisiae*. Appl. Microbiol. Biotechnol. 59, 436–442.